SUPPLEMENTARY INFORMATION

doi:10.1038/nature11516

I. Part Engineering

I.A. Determination of the complete invF gene

The first synthetic *invF* gene was based on the amino acid sequence from the annotated *Salmonella typhimurium* genome (accession number AE006468). This gene failed to induce the *sicA* promoter in the presence of SicA (Fig. 2a and 2b, "Annotated InvF"). There is a long 5'-UTR between the *invF* promoter and the *invF* gene that could be important for regulation. In addition, we noticed that there is an in-frame ATG located 99 bp upstream of the annotated translation start. Three experiments were designed to test the importance of this region. First, six constructs with various lengths of 5'-UTR were made (Fig. S1). The three gates containing both ATGs (ORF1, 2, and 3) worked, whereas the other three constructs containing *invF* with only the downstream ATG (ORF4, 5, and 6) did not. Second, site-directed mutagenesis was performed to generate two different constructs based on the wild-type sequence, starting from each ATG (Fig. S2). The mutation of the upstream ATG (ORF6*; ATG to ACG) would generate the shorter protein, while that of the downstream ATG (ORF1*; ATG to CTG) would result in production of the longer protein containing a changed amino acid residue (M to L). Consistent with our hypothesis, only the longer *invF* ORF1*is functional. Third, the RBS for the shorter ORF was randomized to determine whether the loss of function was due to low expression of the shorter ORF. None of the tested 15 constructs activated the psicA promoter (data not shown).

Interestingly, these dual ATGs are preserved in homologous genes in other species. For example, the *mxiE* gene from *Shigella* was also incorrectly assigned to the downstream gene and then later corrected by Parsot and co-workers[1]. That was a non-trivial discovery because the upstream ATG is out-of-frame and the gene requires transcriptional slippage to express the proper protein. Our synthetic version of this gene includes an additional nucleotide to keep the gene in-frame (Table S4). This is further complicated because not all InvF homologues require this upstream region for function. For example, the *Pseudomonas exsA* gene also has two ATGs separated by 57 nucleotides, but the shorter one is the correct gene and is used in this work[2]. This species diversity and misannotation characterizes the challenge of part mining of transcription factors from sequence databases.

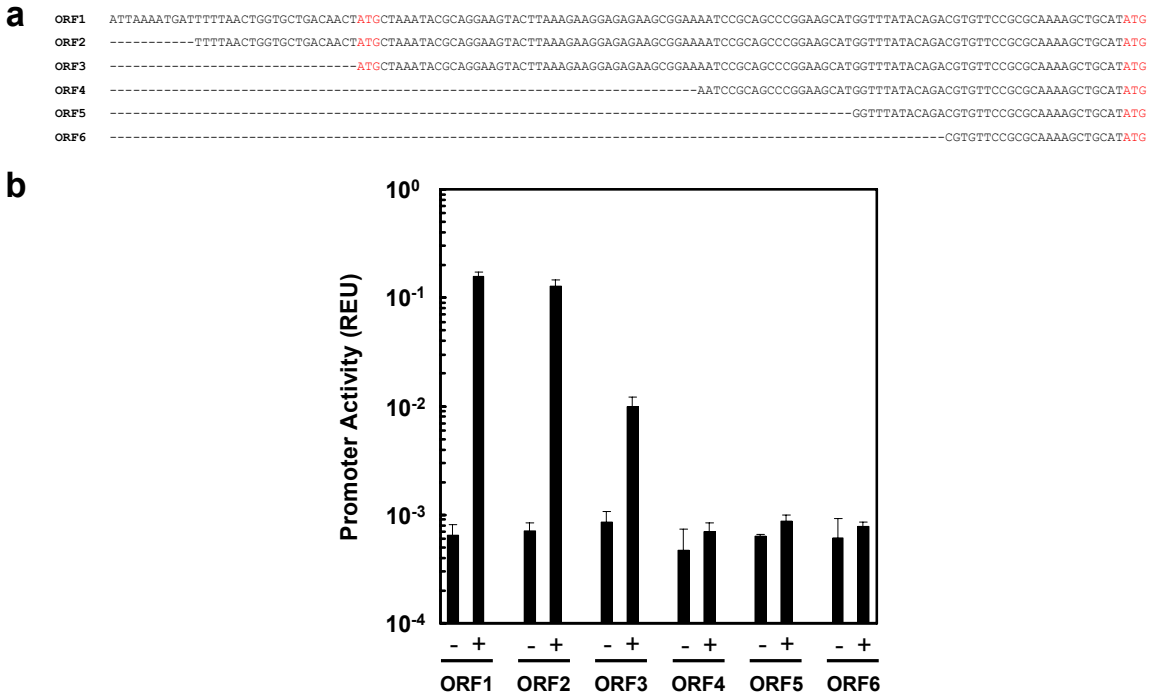

Figure S1: **Comparisons of InvF activity with different truncations of the 5'-UTR. (a)** The different truncated sequences are shown with the up- and downstream ATGs in red. **(b)** The three AND gates containing *invF* ORFs with the upstream ATG (ORF1, 2, and 3) are functional, while the other constructs containing *invF* ORFs with the downstream ATG only (ORF4, 5, and 6) are non-functional. The inducer concentrations used are 5 mM Ara for *sicA* and 100ng/ml aTc for *invF* (+) and no inducers (-). Data are averages and standard deviations of three replicates performed on different days.

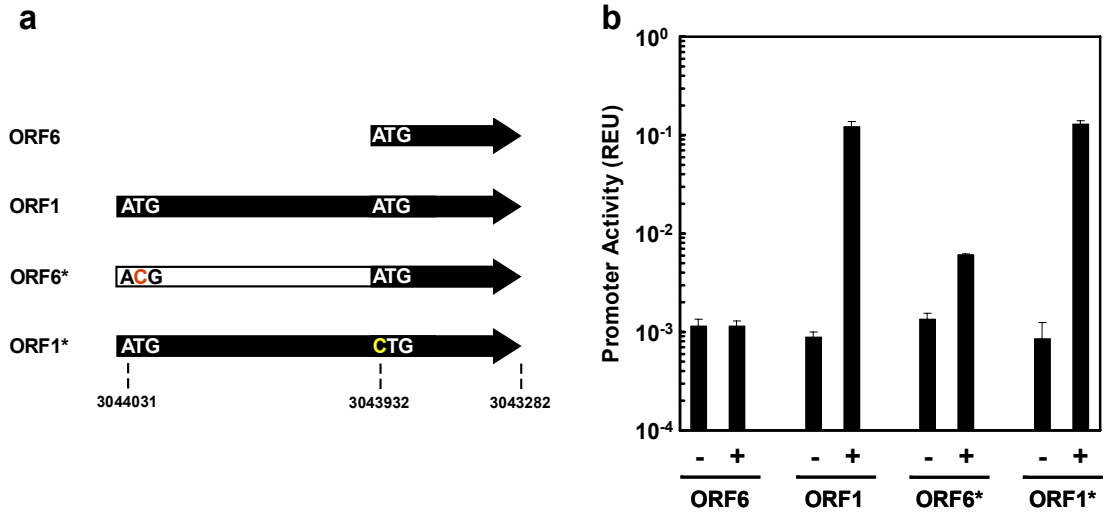

Figure S2: **Mutation of the *invF* start codons. (a)** Site-directed mutagenesis was performed to generate two constructs, starting from each ATG (ORF6* and ORF1*). The numbers are based on sequence from the *Salmonella typhimurium* genome (accession number AE006468) **(b)** The shorter ORFs (ORF6 and 6*) lead to non-functional gates, while the longer ORFs (ORF1 and 1*) yield functional AND gates. The inducer concentrations used are 5 mM Ara for *sicA* and 100ng/ml aTc for *invF* (+) and no inducers (-). Data are averages and standard deviations of three replicates performed on different days.

I.B. Optimization of the dynamic range of promoters

Three promoters used in our circuits (pipaH, pLux, and pTet) were found to have high basal expression levels. To improve their dynamic range, saturation mutagenesis was applied to regions of the promoter, followed by selecting functional AND gates (see Section VII for detailed methods; Fig. S3 and Table S4 for sequences). In addition, the RBSs for *invF*, *ipgC*, and *mxiE* were optimized similarly (Fig. S3).

Saturation mutagenesis was performed on the -10 regions of pipaH and pLux. The RBS libraries for *invF*, *ipgC*, and *mxiE* were constructed by randomizing the bases within 40 bases upstream of the start codons (Fig. S3). The pTet promoter was modified by changing the sequence near the transcription start site and by inserting an additional 20 nucleotides (CAGCAGGACGCACTGACC) upstream of the -35 region. The additional 20 nucleotides were added to better insulate the promoter region from the upstream region[3]. Each plasmid library was used to transform *E. coli* containing the partner plasmids (Table S5). This transformation led to each AND gate library to be screened. Fluorescence was measured from uninduced and induced cultures of each clone, and the clone showing AND logic (high fluorescence only with both inducers) was selected. As summarized in Fig. S3, circuit performance was significantly enhanced by this library-based approach.

For the RBS screening of *invF*, 107 clones were assayed. The parent clone showed 4-fold induction (on to the highest off state), and four variants (4%) showed at least 1.5-fold improvement (at least 6-fold induction). The selected one demonstrated 12-fold induction.

In one library, multiple parts were screened simultaneously (the pipaH promoter and RBSs for *ipgC* and *mxiE*). For the first library, 156 clones containing RBS mutations for both *ipgC* and *mxiE* were assayed. The parent clone showed 1.5-fold induction (on to the highest off), and the best mutant demonstrated 2.6-fold induction. Based on this mutant, pipaH variants were made and one clone (pipaH*) was selected among 109 candidates and demonstrated 7.1-fold induction. Among the 109 clones screened, eleven (10%) showed improved dynamic ranges (at least 3-fold from on to the highest off).

For the AND gate based on the ExsC-ExsDA, the two inducible promoters were modified and screened sequentially. The -10 region of the plux promoter was randomized (Fig. S3), and one clone (plux*) was selected among 95 clones. The original clone (with plux) showed no significant difference in output between the highest off input and the on input [11] state, and the selected one showed 6-fold induction. The screening for pTet variants was followed, and five clones (5% among 94 clones) showed at least 3-fold improvement. The selected one (with pTet*) demonstrated 20-fold induction with both the higher on and lower off states than the parent clone (Fig. S3). Note that this screening was performed using the pexsD promoter, which was replaced with pexsC in the final AND gate because the pexsD promoter was also induced by SicA*-InvF (the same level as that of ExsC-ExsDA) and IpgC-MxiE (~50% of ExsC-ExsDA). The final AND gate (ExsC-ExsDA-pexsC) demonstrated 7-fold induction (on to the highest off).

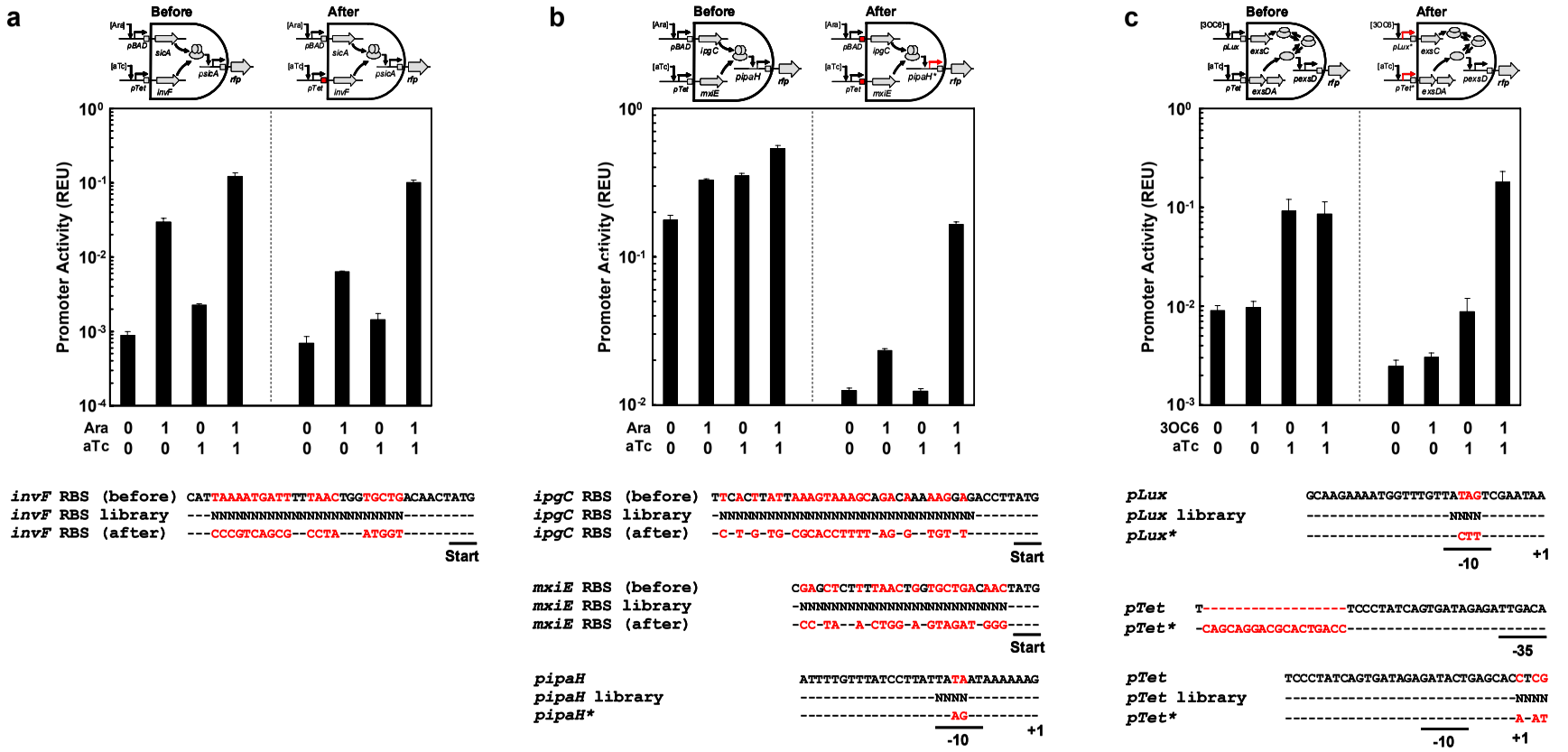

Figure S3: **Directed evolution of promoter and RBS sequences.** AND gates are shown based on **(a)** *Salmonella*, **(b)** *Shigella*, and **(c)** *Pseudomonas* parts. (Top) The architecture of the AND gates. The modified parts are in red. (Middle) A comparison of the constructs before (left) and after (right) part modification. (Bottom) Sequences of the RBS and promoter regions before and after part optimization. Start codons (start) and -10/-35 regions are underlined, different nucleotides are in red, and transcription start sites are indicated by +1. N represents all four nucleotides in the mutagenesis library. The input inducer concentrations used for the on input are 5 mM Ara, 50 ng/ml aTc, and 5 μM 3OC6. Data are averages and standard deviations of three replicates performed on different days.

II. Detailed Data for Circuit Orthogonality

For the gates to be orthogonal, each activator-chaperone pair should only interact with its cognate promoter (Fig. 2e and 2f). Similarly, the chaperones should only interact with their cognate activators. There are 27 possible combinations for three gates consisting of three parts each (activator, chaperone, and promoter). To measure orthogonality, all 27 interactions have been tested using each strain containing different activator-chaperone-promoter combinations (Fig. S4). Each stain was also tested using four inducer conditions ([00], [10], [01], and [11]) as described in Section VII. Strong induction was only observed between cognate partners (87, 14, and 34-fold for psicA, pipaH*, and pexsC, respectively). Weak induction was detected from the following non-partners (Fig. S4): IpgC-InvF-psicA (8.1-fold), SicA*-InvF-pipaH* (2.9-fold), and SicA*-MxiE-pipaH* (2.7-fold).

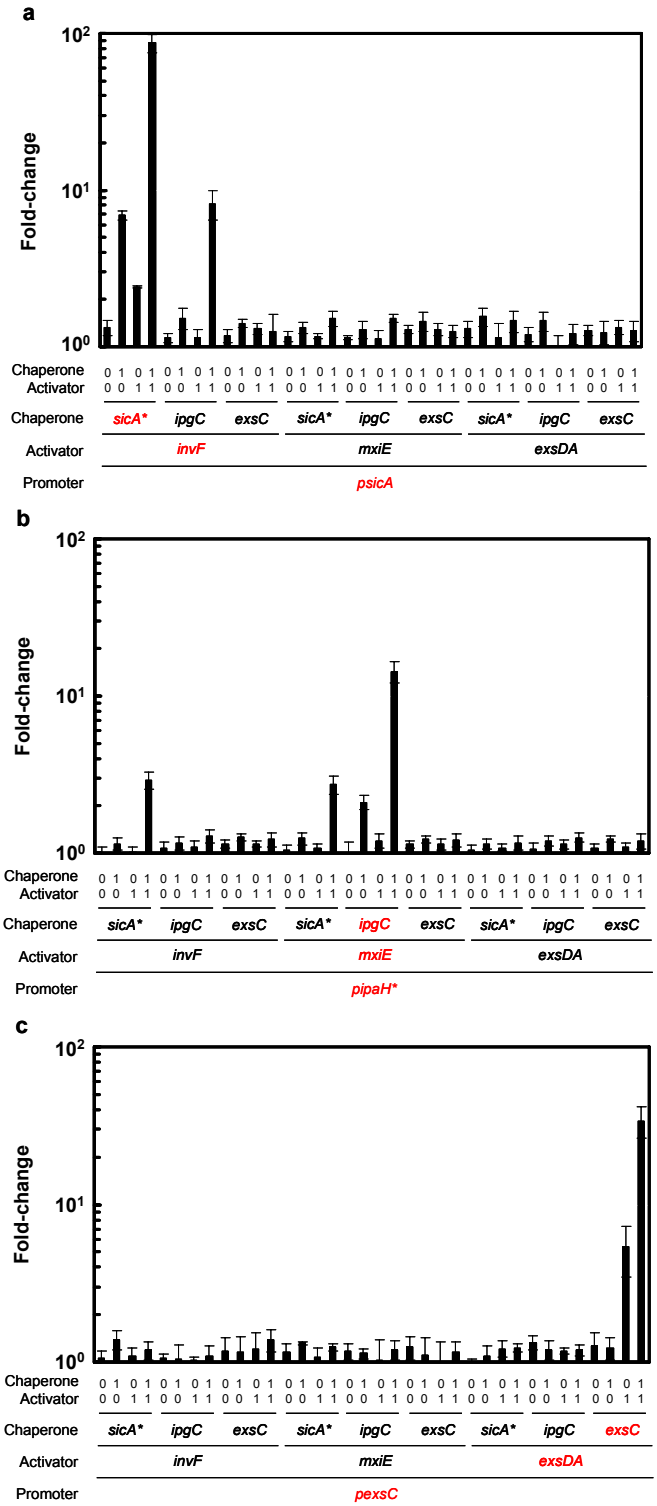

Figure S4: **Enumeration of the interactions between the three 2-input AND gates.** This is an expansion of the data used to generate Fig. 2e and 2f. The data is organized around the activation of the output promoter of each gate (red) as well as its cognate activator/chaperone pair (also in red). Data obtained using **(a)** the psicA promoter, **(b)** the pipaH* promoter, and **(c)** the pexsC promoter. The input inducer concentrations used for the on (1) input are 5 mM Ara for *sicA** and *ipgC*; 1 µM 3OC6 for *exsC*; and 50 ng/ml aTc for *invF*, *mxiE*, and *exsDA*. No inducer is added for the off (0) input. Data are averages and standard deviations of three replicates performed on different days.

Table S1. Fluorescence values (au) for the orthogonality test (Fig. S4).

	Promoter							
	psicA		*pipaH**		*pexsC*			
(Chaperone, Activator)*	Fluorescence (au)	Standard deviation	Fluorescence (au)	Standard deviation	Fluorescence (au)	Standard deviation	Activator	Chaperone
(0, 0)	91	10	443	44	73	8	*invF*	*sicA**
(1, 0)	472	30	505	45	95	13		
(0, 1)	165	2	447	34	75	8		
(1, 1)	5962	789	1294	159	82	11		
(0, 0)	78	5	479	43	72	5		*ipgC*
(1, 0)	104	16	513	52	72	16		
(0, 1)	78	9	481	47	71	2		
(1, 1)	556	118	568	52	75	13		
(0, 0)	81	8	509	30	80	17		*exsC*
(1, 0)	96	6	558	32	80	20		
(0, 1)	89	7	508	23	83	22		
(1, 1)	86	25	542	58	95	15		
(0, 0)	80	6	462	36	79	10	*mxiE*	*sicA**
(1, 0)	91	7	550	50	90	2		
(0, 1)	80	3	474	34	74	11		
(1, 1)	103	11	1210	156	85	5		
(0, 0)	78	2	444	78	80	10		*ipgC*
(1, 0)	88	11	934	101	78	6		
(0, 1)	77	10	533	53	70	24		
(1, 1)	104	6	6360	977	82	12		
(0, 0)	88	5	502	23	85	14		*exsC*
(1, 0)	100	14	542	30	76	22		
(0, 1)	88	8	504	43	69	23		
(1, 1)	86	7	534	51	79	13		
(0, 0)	89	10	463	40	69	3	*exsDA*	*sicA**
(1, 0)	106	14	506	38	75	12		
(0, 1)	78	17	480	26	84	9		
(1, 1)	100	16	516	56	85	5		
(0, 0)	82	8	469	44	92	9		*ipgC*
(1, 0)	100	14	529	39	82	12		
(0, 1)	68	12	503	32	81	3		
(1, 1)	83	12	557	37	82	6		
(0, 0)	87	7	476	29	87	18		*exsC*
(1, 0)	85	14	543	25	85	14		
(0, 1)	91	9	482	30	369	131		
(1, 1)	86	13	529	56	2335	532		

* The input inducer concentrations used for the on (1) input are 5 mM Ara for *sicA** and *ipgC*; 1 μM 3OC6 for *exsC*; and 50 ng/ml aTc for *invF*, *mxiE*, and *exsDA*. No inducer is added for the off (0) input. Data are averages and standard deviations of three replicates performed on different days.

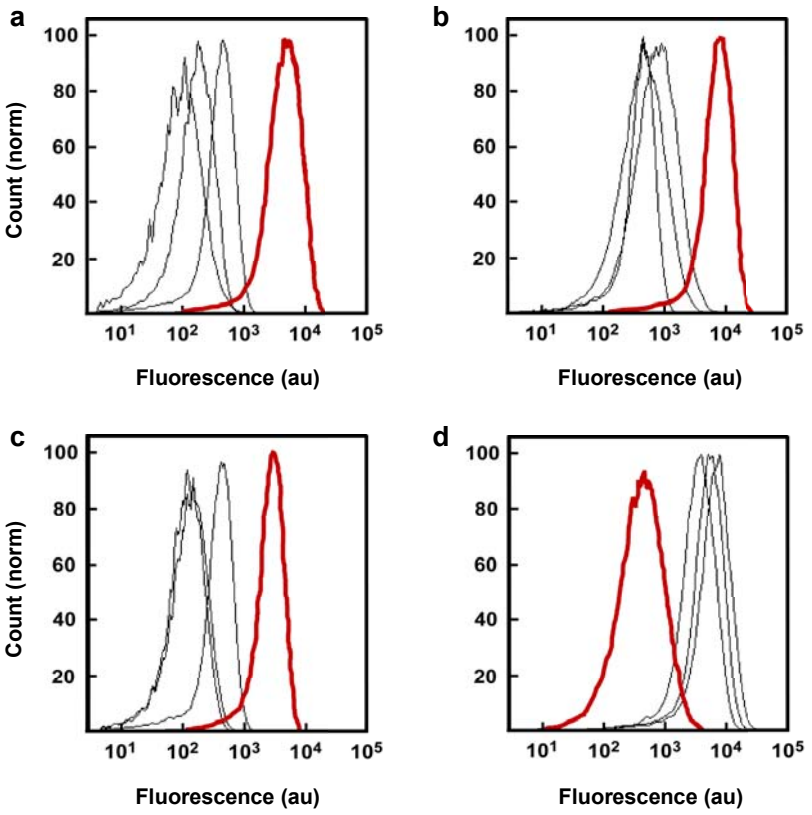

Figure S5: **Raw cytometry data for 2-input gates.** (a) the *Salmonella* AND gate. (b) the *Shigella* AND gate. (c) the *Pseudomonas* AND gate. (d) the NAND gate (Section III). The histograms are shown for all four sets of input states and the thick red line is for the [11] set of inducers. The inducers used for the on input are 25 mM Ara (5 μM 3OC6 for the *Pseudomonas* AND gate) and 50 ng/ml aTc.

III. Construction of NAND Gate

A NAND gate can be constructed by layering an AND and a NOT gate. The 2-input AND gate, built using *Salmonella* parts (Fig. 3), was connected to a NOT gate by inserting a repressor gene *phlF* and its cognate synthetic promoter pphlF between the psicA promoter and *rfp* (Fig. S6). The PhlF sequence was from *Pseudomonas fluorescens* (UniProtKB Accession No. Q9RF02)[4], and the gene sequence was modified for optimal production in *E. coli*. To construct the cognate repressible promoter, the PhlF operator sequence[5] was inserted between the -10 and -35 sequence of a constitutive promoter (BBa_J23119). The -10 sequence of the constitutive promoter was modified to keep the optimal 17 bp spacing between the -10 and -35 sequence (see Table S4 for the synthetic repressible promoter sequence).

The RBS region for the repressor gene *phlF* was modified by saturation mutagenesis. To construct the RBS library, the bases (between -7 and -18 upstream of the start codon ATG; GAAAGGGAGAAA) were randomized using oligonucleotides. The original clone showed no significant difference in output between the lowest off input and the on input [11] state. Among 94 clones screened, eleven (12%) showed improved dynamic ranges (at least 3-fold repression between the lowest off input and the on input [11] state). The selected NAND gate (with the modified RBS sequence CCAATCACTCAT) demonstrates 13- and 7-fold repression below the off input state [00] and the lowest off input state [10] (with the pBAD promoter on), respectively.

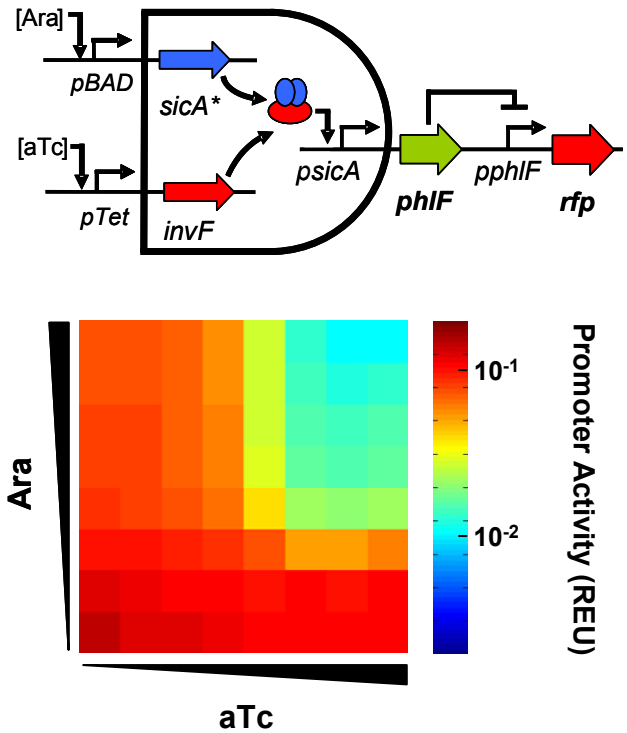

Figure S6: **2-input NAND gate constructed by layering an AND and a NOT gate.** The data were obtained by measuring fluorescence. The inducers used are Ara (0, 0.0016, 0.008, 0.04, 0.2, 1, 5, and 25 mM) from bottom to top; and aTc (0, 0.0032, 0.016, 0.08, 0.4, 2, 10, and 50 ng/ml) from left to right. Data represent averages of three replicates performed on different days.

IV. Mathematical Analysis

IV.A. Transfer Functions of Inducible Systems

The ligand binding to its transcription factor (TF) at equilibrium is described by the equation

$$f_{TL} = \frac{L^n}{K_D{}^n + L^n} \quad , \tag{1}$$

where f_{TL} is the fraction of TF bound to ligand, L is the concentration of ligand, K_D is the dissociation constant, and n is the cooperativity. By mass balance, the fraction of TF without ligand bound f_T is

$$f_T = 1 - f_{TL} \quad . \tag{2}$$

For the promoter pBAD, pTac, pLux, and pTet, the activity of each promoter P_i is described[6-8] by the following equations (Fig. S7 and S8):

$$P_{BAD} = F_{BAD}^{\max}\left(\frac{K_1 + K_2 f_{TL}}{1 + K_1 + K_2 f_{TL} + K_3 f_T}\right) \tag{3}$$

$$P_{Tac} = F_{Tac}^{\max}\left(\frac{K_1}{1 + K_1 + K_2 f_T}\right) \tag{4}$$

$$P_{Lux} = F_{Lux}^{\max}\left(\frac{K_1 + K_2 f_{TL}}{1 + K_1 + K_2 f_{TL}}\right) \tag{5}$$

$$P_{Tet} = F_{Tet}^{\max}\left(\frac{K_1}{1 + K_1 + 2K_2 f_T + K_2{}^2 f_T{}^2}\right) \quad , \tag{6}$$

where $F_i^{\max}$ is the value at maximum induction, measured in fluorescence and reported in REU (relative expression unit; see Section VII for details). The transfer function of each promoter was determined by measuring the expression of RFP (plasmid pBAD-rfp, pTac-rfp, pLux-rfp, pLux*-rfp, pTet-rfp, and pTet*-rfp) at different concentrations of inducer. Parameters were fit using least square minimization to the promoter activity data (Fig. S8) and summarized in Table S2.

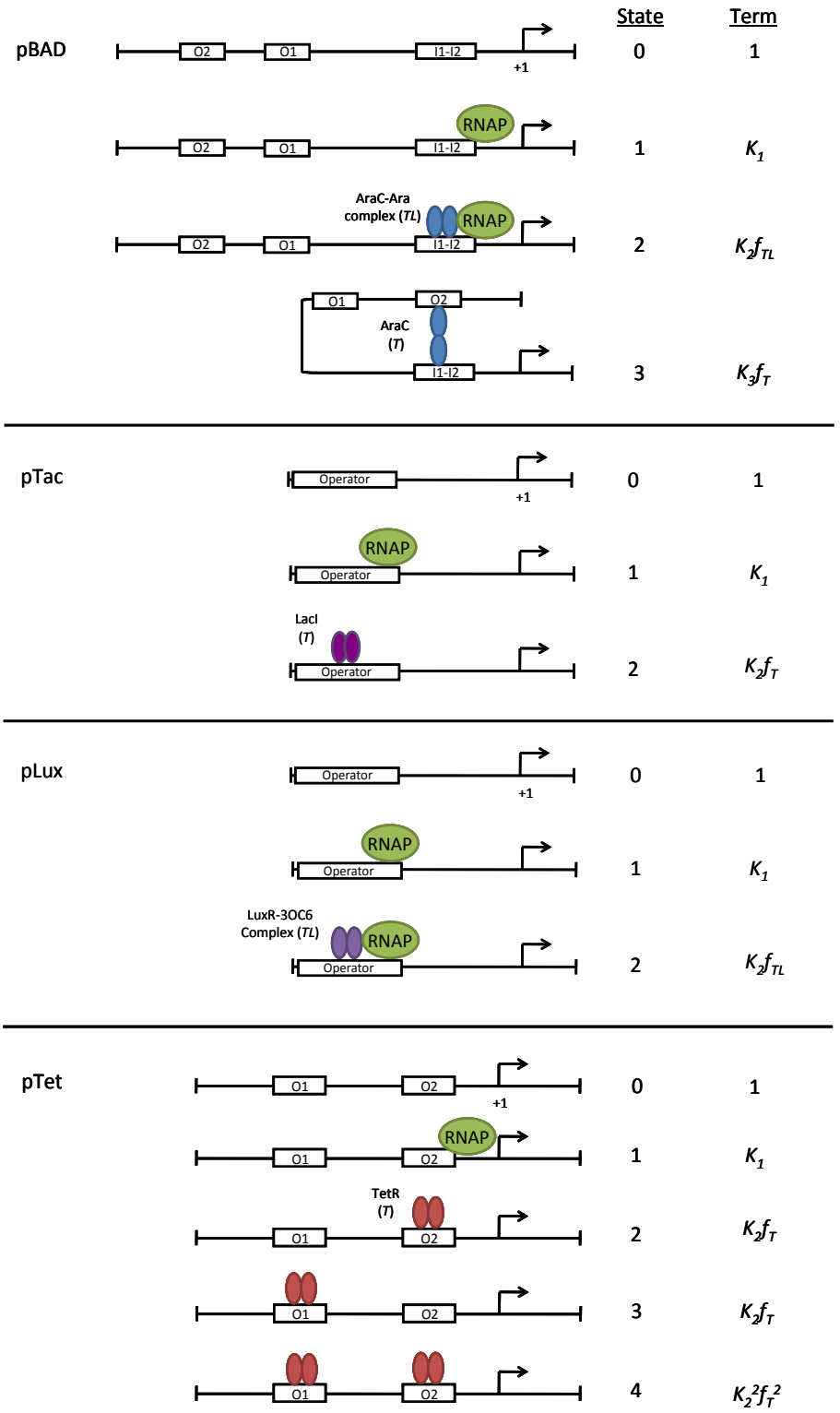

Figure S7: **The binding states of the inducible promoters.** The terms of the partition function for each state are shown on the right column. It is assumed that the RNAP concentration is constant. Some possible states are assumed to be infrequently occupied (not shown). I1-I2, O1, and O2 are operator sites. Binding of AraC-Ara or LuxR-3OC6 complex to its operator site activates its promoter, while binding of AraC, LacI, and TetR represses it.

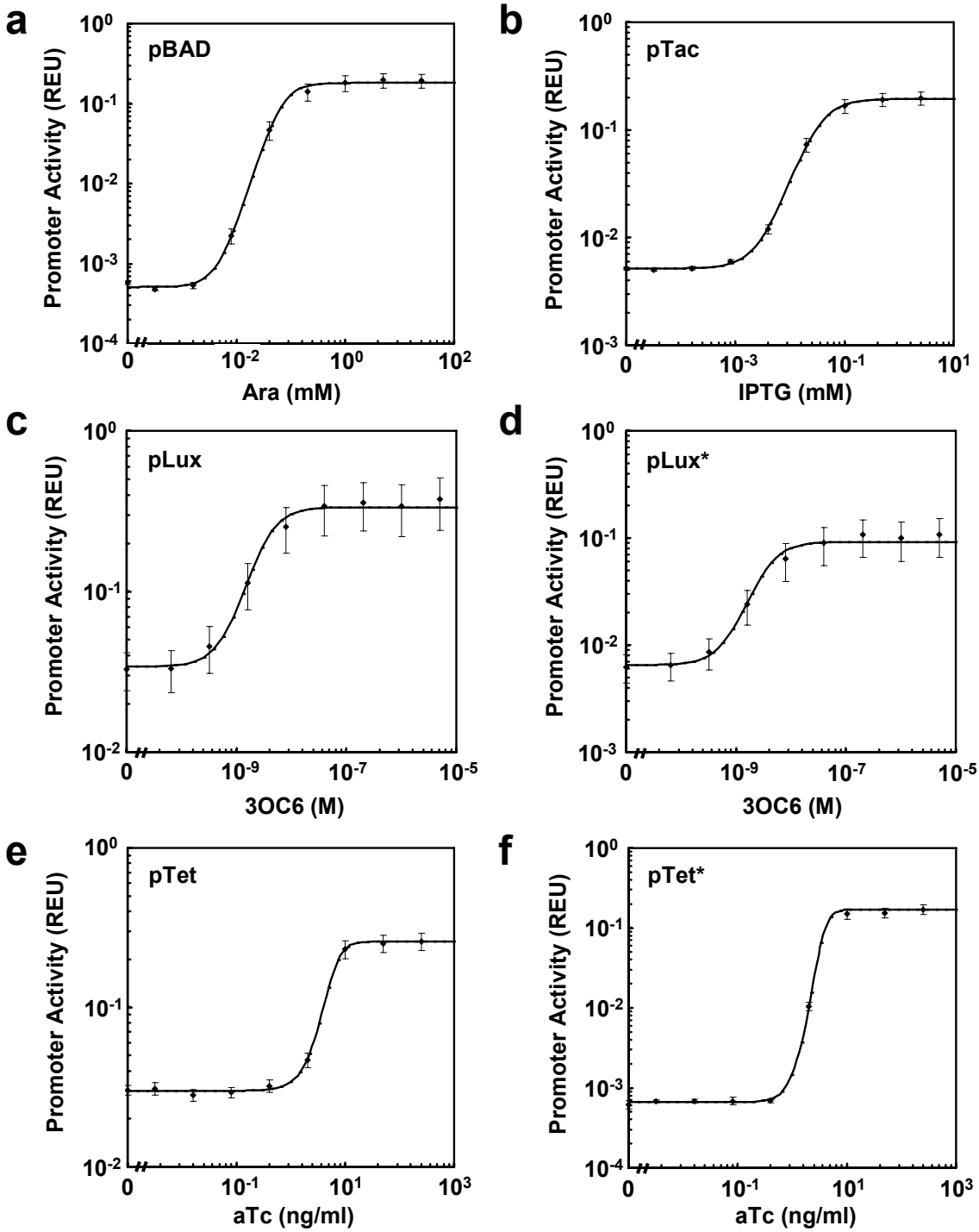

Figure S8: **The transfer functions of the output promoters of the inducible systems.** The transfer function describes how the output varies as a function of input. In this case, this is the promoter activity (measured in fluorescence and reported in REU) and the inducer concentration, respectively. The transfer functions are shown for: **(a)** pBAD **(b)** pTac **(c)** pLux **(d)** pLux* **(e)** pTet **(f)** pTet*. The promoter sequences are summarized in Table S4. Data are averages and standard deviations of three replicates performed on different days. The solid line corresponds to the fit to a model (Equation 3-6 and Table S2).

Table S2. Parameters for input promoters.

	pBAD	pTac	pLux	pLux*	pTet	pTet*
K_D	0.1 mM	0.003 mM	10 nM[a]	10 nM[a]	3.6 ng/ml	1.3 ng/ml
n	2.2	1.6	1.7	1.7	2.0	2.6
K_1	0.014	53	0.10	0.064	350[b]	350[b]
K_2	12	1950	8.3	5.6	51	300
K_3	4.4					
$F_i^{\max}$	0.20	0.20	0.37	0.11	0.26	0.17

a. Parameter was set according to the literature value[9].
b. Parameter was set according to the literature value[10, 11].

IV.B. Transfer Functions of AND Gates

AND gates consisting of activator and chaperone

The production of proteins is modeled as

$$\frac{dA_O}{dt} = \alpha_A \beta_A P_{Tet} - \gamma_A A_O \quad \text{and} \quad (7)$$

$$\frac{dC_O}{dt} = \alpha_C \beta_C P_{BAD} - \gamma_C C_O \quad , \quad (8)$$

where A is activator under the control of the pTet promoter and C is chaperone under the control of the pBAD promoter. It is assumed that chaperones bind to an activator molecule as a dimer[12-15]. A_O and C_O are the total amounts of each protein. α_i is the maximum transcription rate, β_i is protein production rate, and γ_i is the degradation rate. P_i is the activity of promoter i (Equations 3-6). At equilibrium, $[A]$, $[C]$, and $[AC_2]$ are related by the dissociation constant

$$K_{AC} = \frac{[A][C]^2}{[AC_2]} \quad (9)$$

and mass balances

$$A_O = [A] + [AC_2] \quad \text{and} \quad (10)$$

$$C_O = [C] + 2[AC_2] \quad . \quad (11)$$

The values of A_O and C_O at steady state can be estimated from the transfer functions describing the pTet and pBAD promoters:

$$A_O = \frac{\alpha_A \beta_A}{\gamma_A} P_{Tet} = \theta_A P_{Tet} \quad \text{and} \quad (12)$$

$$C_O = \frac{\alpha_C \beta_C}{\gamma_C} P_{BAD} = \theta_C P_{BAD} \quad . \tag{13}$$

In essence, the values of θ_A and θ_C rescale the transfer functions in Fig. S8 in order to account for changes in expression of the genes by various factors including different RBSs. Considering the binding states (Fig. S9a) and Equation 9, the transfer function of the promoter can be written as

$$P_R = k_R \left(\frac{K_1 + K_2[AC_2]}{1 + K_1 + K_2[AC_2]} \right) = k_R \left(\frac{K_1 + \frac{K_2}{K_{AC}}[A][C]^2}{1 + K_1 + \frac{K_2}{K_{AC}}[A][C]^2} \right) \quad , \tag{14}$$

where P_R serves as the output of the gate, is also reported in REU, and is reported as the heat map of Fig. 3c. k_R is a rescaling factor, the ratio of the measured promoter activity (in REU) to the partition function value at the maximum induction.

The promoter activities in Equations 3, 6, 12 and 13 (P_{Tet} and P_{BAD}) serve as the inputs to the gates and are reported in REU. Similarly, the output promoter of the gate (P_R) is reported in REU. Equations 10-14 yield a set of equations that can be solved numerically using the fminsearch minimization routine in MATLAB and fit with the experimental data from the array of inducer combinations (Fig. 3b). The predicted transfer functions (Fig. 3c) are compared with the experimental data (Fig. 3b) and the parameters are summarized in Table S3. The two dimensional data from the model and experiment are also compared in Fig. S10.

Table S3. Parameters for AND gates consisting of activator and chaperone.

	K_1	K_2	K_{AC}	θ_A	θ_C	k_R
Salmonella	1.4×10^{-7}	3.6	5.4×10^{-9}	9.5×10^{-6}	1.1×10^{-3}	1.3×10^{4}
Shigella	2.6×10^{-7}	4.5×10^{2}	4.9×10^{-8}	2.6×10^{-5}	4.1×10^{-5}	2.0×10^{4}

AND gate consisting of activator, antiactivator, and chaperone

The *Pseudomonas* system has a slightly different topology, where ExsA is active alone and is inactivated by ExsD, which is co-transcribed. A third protein ExsC activates ExsA by inhibiting ExsD via a partner swapping mechanism. Thus, all three genes need to be included to build an AND gate. The production of proteins are modeled as

$$\frac{dA_O}{dt} = \alpha_A \beta_A P_{Tet^*} - \gamma_A A_O \quad , \tag{15}$$

$$\frac{dC_O}{dt} = \alpha_C \beta_C P_{Lux^*} - \gamma_C C_O \quad \text{and} \tag{16}$$

$$\frac{dD_O}{dt} = \alpha_D \beta_D P_{Tet*} - \gamma_D D_O \quad , \qquad (17)$$

where D is anti-activator and A is activator under the pTet* promoter control and C is chaperone under the pLux*promoter control. α_i is the maximum transcription rate, β_i is protein production rate, and γ_i is the degradation rate. A_O, C_O, and D_O represent total amount of each protein. At equilibrium, [A], [C], [D], [AD], and [CD] are related by the following equations[16-18]:

$$A_O = [A] + [AD] \qquad (18)$$
$$C_O = [C] + [CD] \qquad (19)$$
$$D_O = [D] + [AD] + [CD] \qquad (20)$$

$$[AD]\, K_{AD} = [A][D] \qquad (21)$$
$$[CD]\, K_{CD} = [C][D] \quad . \qquad (22)$$

A_O, C_O, and D_O can be estimated at steady state using the promoter activities (P_i; Equations 5 and 6):

$$A_O = \frac{\alpha_A \beta_A}{\gamma_A} P_{Tet*} = \theta_A P_{Tet*} \qquad (23)$$

$$C_O = \frac{\alpha_C \beta_C}{\gamma_C} P_{Lux*} = \theta_C P_{Lux*} \qquad (24)$$

$$D_O = \frac{\alpha_D \beta_D}{\gamma_D} P_{Tet*} = \theta_D P_{Tet*} \quad . \qquad (25)$$

Considering the binding states (Fig. S9b), the activity of the promoter pexsC (P_R) is given as

$$P_R = k_R \left(\frac{K_1 + K_2[A] + K_2 K_3 [A]^2}{1 + K_1 + K_2[A] + K_2 K_3 [A]^2} \right) \quad . \qquad (26)$$

Equations 18-26 can be parameterized using the fminsearch function in MATLAB and the experimental data from the array of inducer combinations ($K_1 = 9.7\times10^{-5}$; $K_2 = 6.2\times10^{5}$; $K_3 = 1.0\times10^{7}$; $K_{AD} = 3.3\times10^{-8}$; $K_{CD} = 2.7\times10^{-8}$; $\theta_A = 6.8\times10^{-6}$; $\theta_C = 2.1\times10^{-5}$; $\theta_D = 2.0\times10^{-5}$; $k_R = 0.46$). The predicted transfer function based on this minimization routine is shown in Fig. 3c. The two dimensional data from the model and experiment are also compared in Fig. S10.

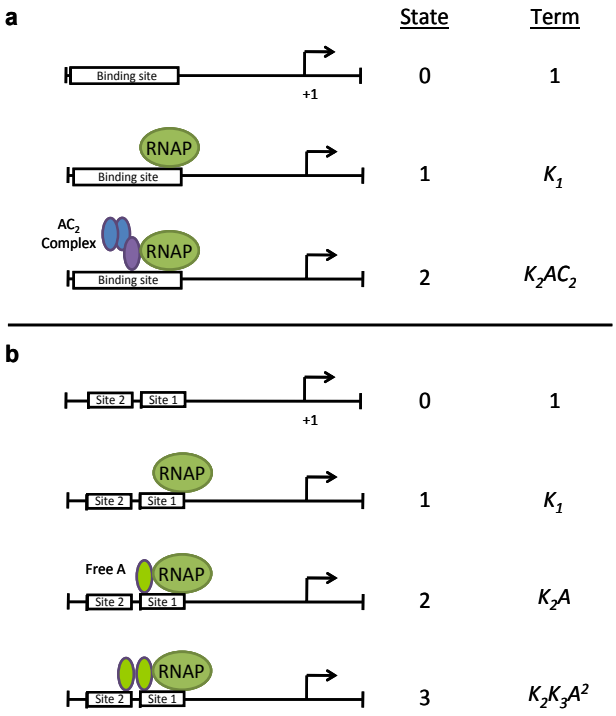

Figure S9: **The binding states of the activator-chaperone complexes binding to their cognate promoters. (a)** The binding states of psicA and pipaH*[12-15]. **(b)** The binding states of pexsC[2, 19, 20].The terms of the partition function for each state are shown on the right column. It is assumed that the RNAP concentration is constant.

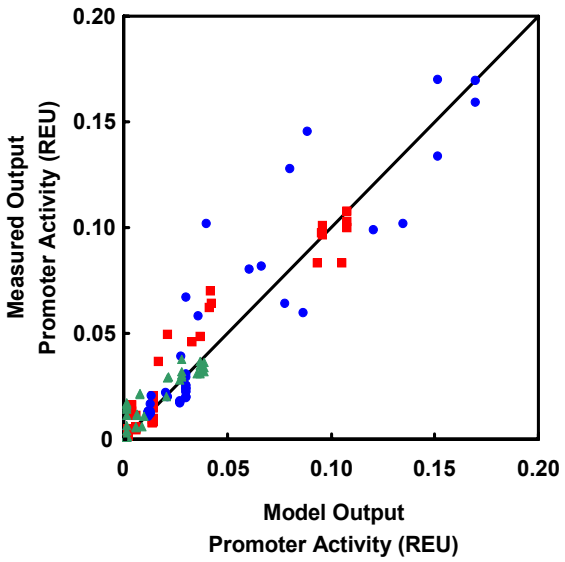

Figure S10: **Comparison between the AND gate model and the experimental data.** Each data point represents the experimental value from the inducer combinations (Fig. 3b), which is compared to the corresponding one from the model (Fig. 3c). The 2-input AND gates from *Salmonella* (■, red), *Shigella* (●, blue), and *Pseudomonas* (▲, green) are shown. The R^2 value is 0.9 with respect to the y=x line.

IV.C. Analysis of the Fault Behavior

Here, we use a simple kinetic model of an AND gate to determine the conditions where a fault will occur. Consider an AND gate that is based on two genes whose gene products (x and y) must bind to create a transcriptional activator (Fig. S11a). The rates of x and y are given by the equations,

$$\frac{dx}{dt} = \alpha_x - \gamma_x x \quad \text{and} \quad (27)$$

$$\frac{dy}{dt} = \alpha_y - \gamma_y y \quad , \quad (28)$$

where α_x and α_y are the expression rates and γ_x and γ_y are the degradation rates. The output of the gate is the production of a gene product (*e.g.*, GFP) and is then given by

$$\frac{dg}{dt} = \alpha_g \left(\frac{Kxy}{1+Kxy} \right) - \gamma_g g \quad , \quad (29)$$

where α_g is the production rate of the output gene, γ_g is the degradation rate, and K is the product of two association constants: one for the x:y complex formation and the other for the complex-promoter binding. At steady-state, the levels of x, y, and g are

$$x_{ss} = \frac{\alpha_x}{\gamma_x} \quad , \quad (30)$$

$$y_{ss} = \frac{\alpha_y}{\gamma_y} \quad \text{and} \quad (31)$$

$$G_{ss} = \frac{Kxy}{1+Kxy} \quad , \quad (32)$$

where $G = g(\gamma_g/\alpha_g)$. Equations 29 can be converted into the dimensionless equation as follows:

$$\frac{dG}{d\tau} = \frac{Kxy}{1+Kxy} - G = \frac{K^* XY}{1+K^* XY} - G \quad \text{where} \quad (33)$$

$$\tau = \gamma_g t \quad , \quad (34)$$

$$X = \frac{x}{x_{ss}} \quad , \quad (35)$$

$$Y = \frac{y}{y_{ss}} \quad \text{and} \quad (36)$$

$$K^* = K x_{ss} y_{ss} = K \frac{\alpha_x \alpha_y}{\gamma_x \gamma_y} \quad . \quad (37)$$

A fault occurs if the input signals switch between two states that correspond to an off output, but they transiently produce an on state (behaving as a pulse). For example, for the circuit above, the transition between inputs states

$$\begin{bmatrix} 0 \\ 1 \end{bmatrix} \longrightarrow \begin{bmatrix} 1 \\ 0 \end{bmatrix}$$

corresponds to x turning on and y turning off. Both of these input states correspond to a zero output state. However, if x turns on more quickly than y turns off, both x and y will be simultaneously present and this can lead to the expression of the output gene. Considering x, y, and G, this transition between input states can be shown at steady-state as:

$$\begin{array}{lll} x=0 & x=x_{ss} & \\ y=y_{ss} & \rightarrow \; y=0 & \text{or} \\ G=0 & G=0 & \end{array} \qquad \begin{array}{lll} X=0 & X=1 & \\ Y=1 & \rightarrow \; Y=0 & \\ G=0 & G=0 & \end{array}$$

This transition can be visualized on a simple phase space diagram (Fig. S11b). If the transition occurs entirely along the x axis, then there will be no fault. However, if the trajectory leaves the x-axis, then a fault will occur (dotted line). The magnitude of the fault will correspond to the slope of the trajectory from the origin. This can be determined by taking the derivative at the origin

$$\left.\frac{d}{dX}\left(\frac{dG}{d\tau}\right)\right|_{X\to 0} = \left.\frac{K^{*}Y}{(1+K^{*}XY)^{2}}\right|_{X\to 0} = K^{*}Y\big|_{Y\to 1} = K\frac{\alpha_x\alpha_y}{\gamma_x\gamma_y} \quad . \qquad (38)$$

at steady state. Larger initial slopes correspond to larger faults, so the condition for the occurrence of a fault is

$$K\frac{\alpha_x\alpha_y}{\gamma_x\gamma_y} >> 0 \quad . \qquad (39)$$

This is the solution for when the switch between states is instantaneous. The likelihood for a fault increases when there are delays in one signal as it propagates through additional layers. This corresponds to the following transition,

$$\begin{array}{lll} x=0 & x=x_{ss} & x=x_{ss} \\ y=y_{ss} & \xrightarrow[t_d]{} \; y=y_{ss} & \longrightarrow \; y=0 \\ G=0 & G>0 & G=0 \end{array}$$

where t_d is the delay time before the signal to y occurs, triggering its decay. This leads to the transient intermediate state where both x and y co-exist and the output is on. This can be visualized as a phase diagram (Fig. S11c), where the trajectory begins toward the higher steady-

state for G, and then after t_d, the steady-state switches and the trajectory continues to the lower steady state. The dimensionless timescale τ_c for the initial trajectory from the origin is given by

$$\tau_c = t_c\gamma_g = \frac{1}{\frac{d}{dY}\left(\frac{dG}{d\tau}\right)\Big|_{Y\to 0}} = \frac{1}{\frac{K^*X}{(1+K^*XY)^2}\Big|_{Y\to 0}} = \frac{\gamma_x\gamma_y}{K\alpha_x\alpha_y} \quad . \qquad (40)$$

The condition for a fault can then be written as a comparison between the timescale for the initial trajectory (t_c) and the timescale for the delay (t_d)

$$t_d >> t_c \qquad \text{or} \qquad (41)$$

$$t_d >> \frac{\gamma_x\gamma_y}{K\alpha_x\alpha_y\gamma_g} \quad . \qquad (42)$$

Equation 42 yields a condition for which a fault will occur when there is a delay before the signal reaches y that then causes the degradation of y. One can easily show that no fault will occur for this transition when the delay in the signal affects a production rate (in this case, x).

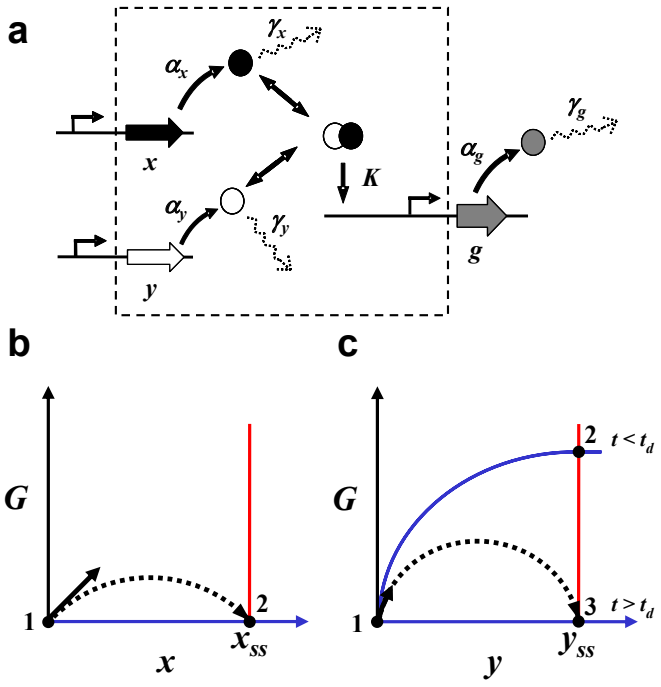

Figure S11: **Analysis to identify scaling conditions for the occurrence and magnitude of faults.** (a) Schematic of the model system. (b) A phase space diagram for the instantaneous transition. The blue and red lines represent the null clines in the system. The circles marked 1 and 2 indicate the stable steady-state before and after the transition, respectively. The dashed curve indicates an example trajectory between states, and the straight arrow shows the slope of the trajectory at the origin. (c) A phase space diagram with the delay time. The trajectory begins towards the higher steady-state for G (position 2), and then after t_d, the steady-state switches and the trajectory continues to the lower steady state (position 3).

V. Dynamic Behavior of the Gates

Genetic programs consisting of layered transcriptional circuits could lead to delays[21]. Time course experiments were performed on all of the 2-, 3-, and 4-input gates (Fig. S12) and all the 16 inducer conditions for the 4-input program (Fig. S13). The cultures were induced at OD_{600} of 0.5 (t = 0) with inducers of representative concentrations as indicated in Fig. S12 and S13. Each culture (0.6 ml) was induced up to 12 hrs in 96-well plates with gas permeable sealing membrane, and flow cytometer data were obtained.

The 2-input AND gates constructed from *Salmonella* and *Pseudomonas* reached the half maximal output in ~2 hrs, while the 3- or 4-input AND gate led to ~1 hr delay in output when compared to that of those 2-input gates. Interestingly, the 2-input AND gate from *Shigella* also showed such delay by ~1 hr. The AND gate from *Pseudomonas* has a different topology and is the fastest among the three 2-input AND gates. Although it is unclear why the 2-input AND gate from *Shigella* responded to the inputs more slowly, such delay could contribute to the slower response of the 3- or 4-input AND gate. There is no significant difference in the temporal behavior between 3- and 4-input AND gate. Note that there is no significant difference in the growth rate between the gates (see Section VI).

The cultures seem to reach steady state after 6-8 hr induction. Up to 12 hrs, the signal remained at the steady state values (Fig. S13). This implies that the stationary cells robustly kept their output signal for several hours after they reached the stationary phase. After 5h induction, the output of the [1111] state was always at least five times higher than any other off state (note that the output of [1111] is 5.1-fold above the highest off state [1011] at 6h when the one-time point experiment was done; Fig. 4e). The each fold difference between [1111] and any individual off state remained similar from 6 to 12h. Considering this, cells were induced for 6 hrs to obtain all the static data points in this study.

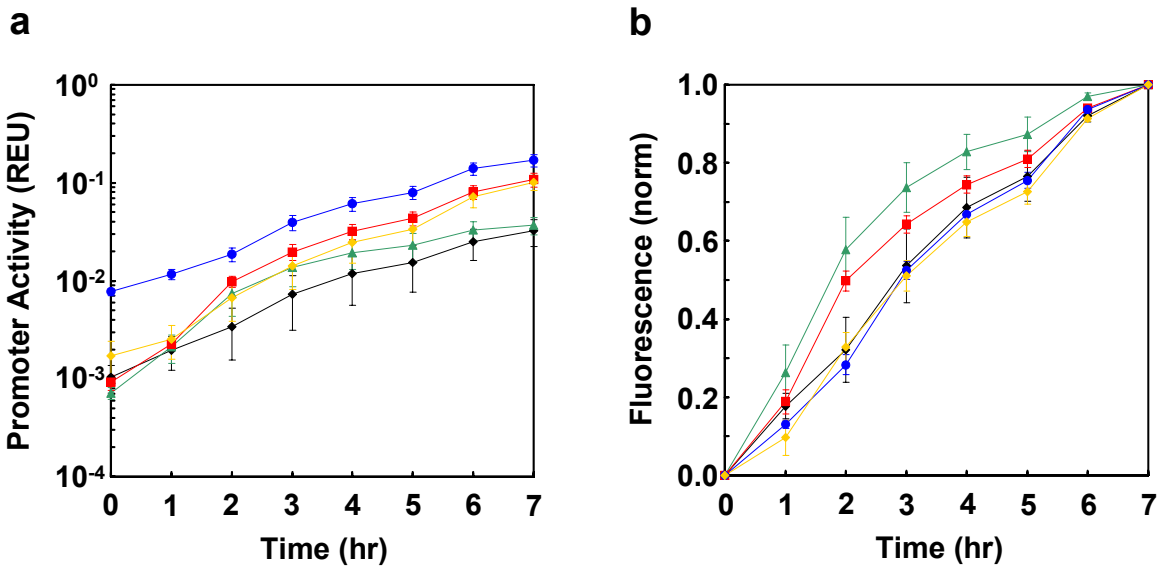

Figure S12: **Temporal behavior of the individual and combined AND gates.** The 2-input AND gate from *Salmonella* (■, red), *Shigella* (●, blue), and *Pseudomonas* (▲, green); the 3-input AND gate (♦, orange); and the 4-input AND gate (♦, black). **(a)** Data are shown in fluorescence (REU). **(b)** Data are normalized by the following formula: $[\log(F) - \log(F_{Min})] / [\log(F_{Max}) - \log(F_{Min})]$ where F, F_{Min}, and F_{Max} are sample, minimum, and maximum fluorescence levels, respectively. The time course is shown after inducers are added at time = 0. All the experiments were performed with the following four inducers added to each culture: Ara (5 mM), IPTG (0.1 mM), 3OC6 (5 μM), and aTc (10 ng/ml). Data are averages and standard deviations of three replicates performed on different days.

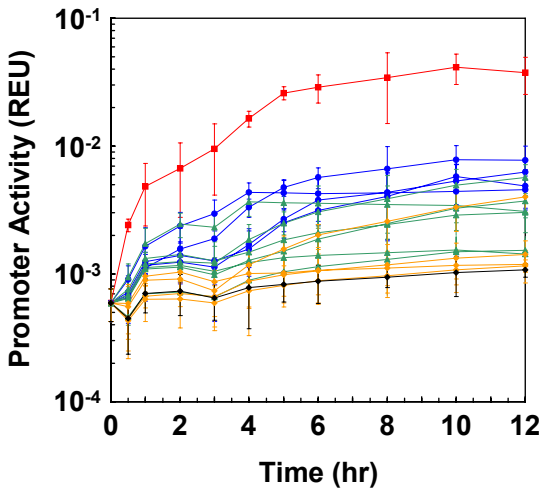

Figure S13: **Temporal behavior of the 4-input AND gate with different inducer combinations.** [0000] (♦, black); [0001], [0010], [0100], and [1000] (♦, orange); [0011], [0101], [0110], [1001], [1010], and [1100] (▲, green); [0111], [1011], [1101], and [1110] (●, blue); [1111] (■, red). The four inducers used for the on input are Ara (5 mM), IPTG (0.1 mM), 3OC6 (5 μM), and aTc (10 ng/ml).

VI. Effect of Gates and Programs on Cell Growth

The effect of the AND gates on cell growth was determined. Each culture (0.6 ml) was induced at OD_{600} of 0.5 (t = 0) with both inducers of representative concentrations as indicated in Fig. S14. Each culture was grown for 7 hrs in 96-well plates (2 ml 96-well deep well plate) with gas permeable sealing membrane, and OD_{600} was measured every hour. There is no significant difference in growth between cells containing different gates (Fig. S14). No significant difference in OD_{600} was observed between uninduced and induced cultures.

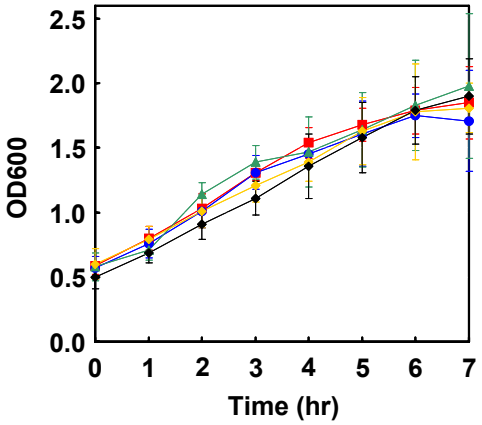

Figure S14: **The effect of the AND gates on cell growth is minimal.** The 2-input AND gate from *Salmonella* (■, red), *Shigella* (●, blue), and *Pseudomonas* (▲, green); the 3-input AND gate (♦, orange); and the 4-input AND gate (♦, black). The time course is shown after inducers are added at t = 0. All the experiments were performed with the following four inducers added to each culture: Ara (5 mM), IPTG (0.1 mM), 3OC6 (5 μM), and aTc (10 ng/ml). Data are averages and standard deviations of three replicates performed on different days.

VII. Materials and Methods

Strains, plasmids, and growth media

E. coli strain DH10B [F^- *mcr*A Δ(*mrr-hsd*RMS-*mcr*BC) Φ80*lac*ZΔM15Δ*lac*X74 *rec*A1 *end*A1 *ara*Δ139 Δ(*ara*, *leu*)7697 *gal*U *gal*K λ-*rps*L (Str^R) *nup*G] was used for all the experiments and grown in LB (Miller, BD Biosciences, San Jose, CA). Kanamycin (20 μg/mL), ampicillin (100 μg/mL), and chloramphenicol (34 μg/mL) were added as appropriate. Four inducers used in this study were obtained from Sigma Aldrich (St. Louis, MO) and the concentration range is as follows: Ara (Arabinose; 320 nM to 25 mM), IPTG (Isopropyl β-D-1-thiogalactopyranoside; 32 nM to 2.5 mM), 3OC6 (*N*-(β-Ketocaproyl)-L-homoserine lactone; 64 pM to 5 μM), and aTc (Anhydrotetracycline; 3.2 pg/ml to 250 ng/ml). Gene synthesis (*invF*, *ipgC*, *mxiE*, *sycB*, *ysaE*, and *phlF*) with codon optimization was performed by DNA 2.0 (Menlo Park, CA), GenScript (Piscataway, NJ), and Life Technologies (Grand Island, NY). For codon optimization, Gene Designer 2.0 (DNA 2.0, Menlo Park, CA) was used. All the genes from *Pseudomonas aeruginosa* (*exsC* and *exsDA*) were cloned from genomic DNA of the strain PAO1 (ATCC 47085) and *sicA* was obtained from Temme *et al*[22]. All the gene sequences are shown in Table S4. All the newly constructed plasmids were made by the one-step isothermal DNA assembly method as described by Gibson *et al*[23] and were summarized in Table S5 and Fig. S15-S18.

Part Mutagenesis

RBS regions were modified by saturation mutagenesis. To construct the RBS libraries for *invF*, *ipgC*, and *mxiE*, the bases (within 40 bases upstream of the start codons) were randomized using oligonucleotides (Integrated DNA Technologies, Coralville, IA) as shown in Fig S3. The oligonucleotide primers were designed to contain random nucleotides (Ns) and were 5'-phosphorylated. After plasmid amplification by PCR reactions using Phusion High-Fidelity DNA polymerase (New England BioLabs, Ipswich, MA), the reaction mixtures were treated with *Dpn*I (New England BioLabs, Ipswich, MA) to digest the template plasmid. The blunt ends were ligated using T4 DNA Ligase (New England BioLabs, Ipswich, MA) to give the mixture of the modified plasmids. This plasmid mixture was used to transform *E. coli* DH10B.

The plasmid library pools, isolated from successful transformant clones, were used to transform *E. coli* DH10B containing the corresponding partner genes and promoters (i.e. *sicA* and psicA for the RBS library for *invF*; *mxiE* and pipaH for the RBS library for *ipgC*; *ipgC* and pipaH for the RBS library for *mxiE*). The resultant transformant clones were transferred into 96-well plates (2 ml 96-well deep well plate, USA Scientific, Orlando FL) with gas permeable sealing membrane (USA Scientific, Orlando FL). Each clone was grown in LB medium overnight at 37°C and then transferred to fresh LB medium. The culture (0.6 ml) at OD_{600} of 0.5 was induced with 5mM Ara and/or 100 ng/ml aTc for 6 hrs. Flow cytometer data were obtained from uninduced and induced cultures, and the clones showing AND logic (with the on output being at least 5-fold above the highest off level) were selected. For the RBS screening for *invF*, *ipgC*, and *mxiE*, 107, 156, and 156 clones were assayed, respectively.

The same procedure was followed for promoter engineering. The -10 regions of pipaH and pLux were randomized, and the region near the transcription start site (+1) of pTet was modified (Fig. S3). The plasmid library pools were used to transform *E. coli* DH10B containing the corresponding partner genes and promoters (i.e. *ipgC* and *mxiE* for the pipaH-rfp library; *exsDA* and pexsD for the pLux-exsC library; *exsC* and pexsD for the pTet-exsDA library). The resultant transformant clones were grown and analyzed as described above. For the induction of the pLux promoter, 5 μM 3OC6 was used. Of the 109, 95, and 94 promoters screened, pipaH*, pLux*, and pTet* were selected, respectively.

The modified plasmid, selected from the screening, was purified from their partner plasmids. The three plasmids from the selected clone AND18 (see Table S5) were isolated using QIAprep Spin MiniPrep Kit (Qiagen, Valencia, CA) after overnight culture in LB supplemented with kanamycin (20 μg/mL) only. The isolated plasmid pTet-invF (containing kanamycin resistance gene), which is contaminated with pBAD-sicA and psicA-rfp, was used to transform *E. coli* DH10B. These transformants were grown on LB agar supplemented with Kanamycin (20 μg/mL) only. Several single colonies were tested for contamination by growing them in LB supplemented with ampicillin (100 μg/mL) or chloramphenicol (34 μg/mL). The purified plasmid pTet-invF was used to determine the modified RBS sequence. Similarly, pBAD-ipgC, pTet-mxiE, and pipaH*-rfp were purified from each other using LB supplemented with the corresponding antibiotics only (100 μg/mL ampicillin, 20 μg/mL Kanamycin, and 34 μg/mL chloramphenicol, respectively). pLux*-exsC and pTet*-exsDA were also purified using LB supplemented with the corresponding antibiotics only (100 μg/mL ampicillin and 20 μg/mL kanamycin, respectively).

Testing orthogonality

Cross-talk was examined after the three functional AND gates had been constructed. The test strain contains three plasmids: one with activator gene, another with chaperone gene, and the other with promoter from T3SS and *rfp* (Table S5). Three AND gates and three interaction components (i.e. three plasmids) gives 27 combinations (AND24, 32, 33, 36-40, 53, 54, 58, 59, 61, 62, 64, 65, 67, 68, and 72-80; for the strain/plasmid information, see Table S5). Each *E. coli* DH10B strain was transformed with three plasmids, and the resultant 27 strains were transferred into 96-well plates (2 ml 96-well deep well plate, USA Scientific, Orlando FL) with gas permeable sealing membrane (USA Scientific, Orlando FL). Each clone was grown in LB medium overnight at 37°C and then transferred to fresh LB medium. The culture (0.6 ml) at OD_{600} of 0.5 was induced for 6 hrs and flow cytometer data were obtained from uninduced and induced cultures (Fig. S4). The input inducer concentrations used for the on input are 5 mM Ara for *sicA** and *ipgC*; 1 μM 3OC6 for *exsC*; and 50 ng/ml aTc for *invF*, *mxiE*, and *exsDA*. No inducer is added for the off input.

Directed evolution of *sicA*

To obtain *sicA* variants, error-prone PCR was performed and a library of SicA mutant proteins was screened as follows. Random mutations were introduced by PCR reactions which were performed using 1x PCR buffer (Invitrogen, Carlsbad, CA) supplemented with 7 mM $MgCl_2$, 0.3 mM $MnCl_2$, 0.2mM of dATP and dGTP, 1mM of dCTP and dTTP, and 0.05U Taq DNA polymerase (Invitrogen, Carlsbad, CA). Strains containing the mutated *sicA* gene, the *invF* gene, and psicA promoter were screened, and 92 positive clones with equivalent or higher fluorescence (when compared to a positive control that contains wild type *sicA*-*invF*-psicA) were selected at 5 mM Ara and 100 ng/ml aTc. The selected *sicA* mutant genes were transformed into strains containing *mxiE* and the pipaH* promoter, and the negative clone (containing SicA*) with activation of lower than 3-fold was selected. For this negative selection, no inducer was added for the off state, and 5 mM Ara and 100 ng/ml aTc were added for the on state.

Flow cytometry

E. coli containing the AND gate was grown in LB medium overnight at 37°C and then transferred to fresh LB medium. The cultures were induced at OD_{600} of 0.5 with inducers of different concentrations as indicated. Each culture (0.6 ml) was induced for 6 hrs in 96-well plates (2 ml 96-well deep well plate, USA Scientific, Orlando FL) with gas permeable sealing membrane (USA Scientific, Orlando FL), and flow cytometer data were obtained (6 hr induction) using a BD Biosciences LSRII flow cytometer equipped with blue (488 nm) and yellow/green (561 nm) lasers (BD Bioscience, San Jose, CA). Samples were diluted using phosphate buffered saline (pH 7) supplemented with 2 mg/ml kanamysin. Injection volume and flow rate were 10 μl and 0.5 μl/s, respectively. For the analysis of the NAND gate, *E. coli* was grown in LB medium to OD_{600} of 0.5 and transferred to fresh LB medium containing inducers (to give OD_{600} of 0.005). Each culture (0.6 ml) was induced for 14 hrs in 96-well plates, and flow cytometer data were obtained as described above.

All the data were gated by forward and side scatter, and each data consists of at least 10,000 cells. The arithmetic mean fluorescence was calculated using FlowJo (TreeStar Inc., Ashland, OR), and the averages of means were obtained from three replicates performed on different days. Every histogram showed only one peak and the arithmetic mean accurately reflects the population (*i.e.*, the distribution is not significantly skewed). Note that the all-or-

nothing behavior of the pBAD promoter[24] was only observed in the characterization of pBAD-rfp at the transition point (0.04 mM Ara in our measurement for Fig. S8a), and the population heterogeneity does not affect the fit to the transfer function model[25]. The multi-population behavior was not observed in the histograms of the multi-input logic gates.

For the characterization of the induction and relaxation of the 4-input program (Fig. 5a), the 8 hr cultures, uninduced or induced with the four inducers (5 mM Ara, 0.1 mM IPTG, 5 μM 3OC6, and 10 ng/ml aTc), were centrifuged and resuspended (to an OD_{600} of 0.25 or 0.05, respectively) with fresh medium containing the four inducers (5 mM Ara, 0.1 mM IPTG, 5 μM 3OC6, and 10 ng/ml aTc) or no inducer. Similarly, for the inducer-switching experiments (Fig. 5c and 5d), the 8 hr cultures, induced with the first inducers (5 mM Ara and 0.1 mM IPTG for the 3-input AND gate; 5 mM Ara, 0.1 mM IPTG, and 5 μM 3OC6 for the 4-input AND gate), were centrifuged and resuspended (to an OD_{600} of 0.25) with fresh medium containing the second inducers (0.1 mM IPTG and 10 ng/ml aTc for the 3-input AND gate; 0.1 mM IPTG, 5 μM 3OC6, and 10 ng/ml aTc for the 4-input AND gate) to eliminate the first inducers from the medium. The resuspended cells were grown for another 6 hrs and their fluorescence was measured every 30 min as described above.

Calculation of Relative Expression Units (REUs)

The fluorescence level produced by the plasmid pStd-rfp (Fig. S15) was used to calculate a relative expression unit (REU)[26]. This is simply a linear factor that rescales the arbitrary units measured by the flow cytometer. The objective of normalizing to REU is to standardize measurements between projects and labs. The linear factor is 2.2×10^{-5} and division by this number converts back to the raw arbitrary units. This number was calculated to be a proxy to the relative promoter units (RPUs) reported by Kelly et al[27]. Our original standardized measurements involved a different reference promoter, RFP, RBS, and plasmid backbone (the plasmid pStd-rfp). Because of this difference, RPUs cannot be calculated as defined by Kelly et al. Instead, a series of plasmids was made to estimate relative expression of reporter proteins from experimental constructs, which was compared with the standard construct in the work of Kelly et al[27]. Conversion factors between constructs were measured and multiplied to obtain the linear factor (Fig. S15)[26]. We renamed the unit REU because it is intended to be a simple normalization of fluorescent units (akin to a fluorescent bead) and not a direct measurement of the activity of a promoter (e.g., polymerase flux).

For our original standardized measurements, *E. coli* containing the pStd-rfp plasmid was grown in LB medium overnight at 37°C and then transferred to fresh LB medium. The 0.6 ml culture at OD_{600} of 0.5 was grown for additional 6 hrs in 96-well plates (2 ml 96-well deep well plate, USA Scientific, Orlando FL) with gas permeable sealing membrane (USA Scientific, Orlando FL), and flow cytometer data were obtained. The sequence of the internal standard promoter is based on that of BBa_J23108 (http://partsregistry.org/Part:BBa_J23108).

[Portions of this methods section have been previously published and reproduced with permission[26]]

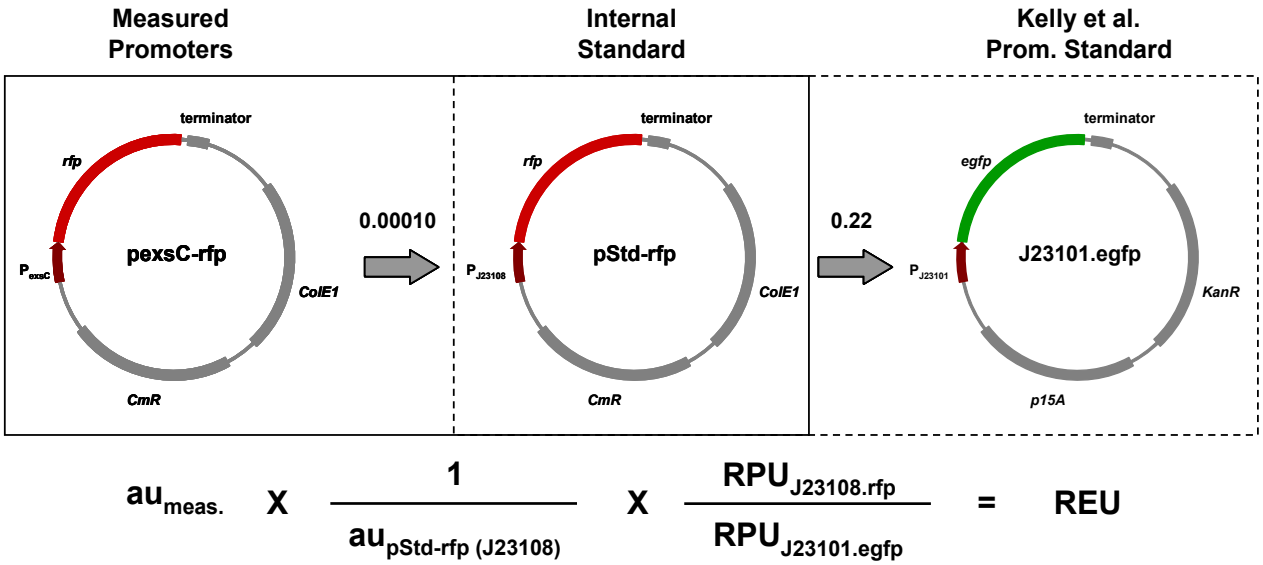

Figure S15: **Conversion of arbitrary units into relative expression units (REUs).** All the promoters (e.g. pexsC) were characterized using RFP in plasmid backbone containing the ColE1 origin and chloramphenicol resistance gene. Data were first normalized by the fluorescence of pStd-rfp (the internal standard). To compare our measurement to expression levels of the Kelly et al. standards[27], the normalized values were further multiplied by the ratio (0.22) of fluorescence by the J23108 promoter to that of the Kelly et al. J23101.egfp standard plasmid. The solid and dashed boxes indicate which plasmids were measured at different facilities.

Calculation of expected output promoter activities for the programs

The transfer functions (Section IV), parameterized using the fluorescence data, were used to calculate the expected output promoter activity of the 3-input (with 8 different input combinations) and the 4-input AND gate (with 16 different input combinations). First, the promoter activity values (P_i) were calculated using Equations 1-6 for both on and off inputs. From Equations 9-14 (for the 3- and 4-input gates) and 18-26 (for the 4-input gate), the output promoter activity P_R (for the first layer) was calculated by using those values (two values) from Equations 1-6 as inputs (P_i). This calculation generated four output values from the first layer gate each. It also enables the experimental ranges to be drawn in Fig. 3c. Second, these output promoter activity values (from the first layer) were used as inputs to repeat the similar calculation, generating the final expected output promoter activities from the second layer. These calculated values are compared with those of the experiments (Fig. 5b). The R^2 value was calculated with respect to the y = x line.

VIII. Strains, Plasmids, and Part Sequences

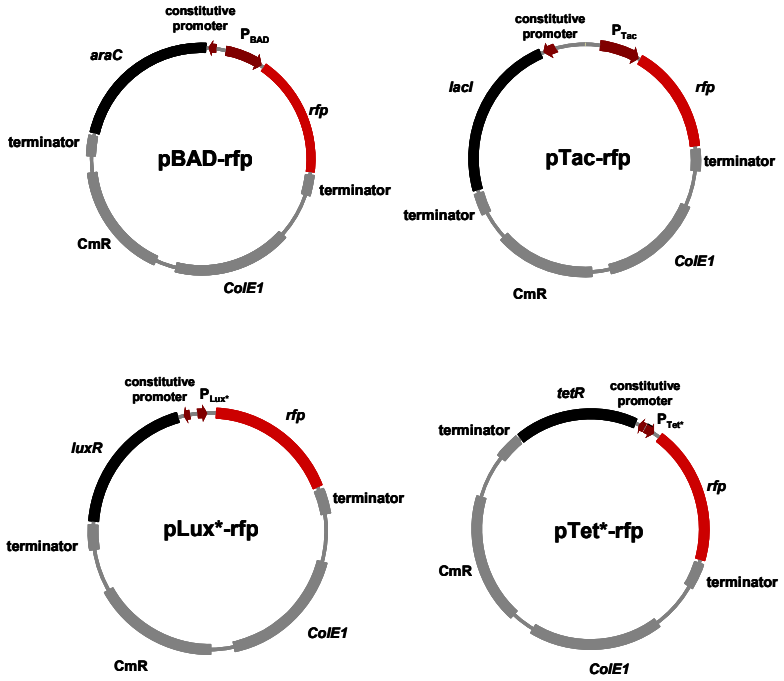

Figure S16: **Plasmids used for 1-D transfer function determination.** The plasmid maps for pLux-rfp and pTet-rfp are the same as those of pLux*-rfp and pTet*-rfp, respectively.

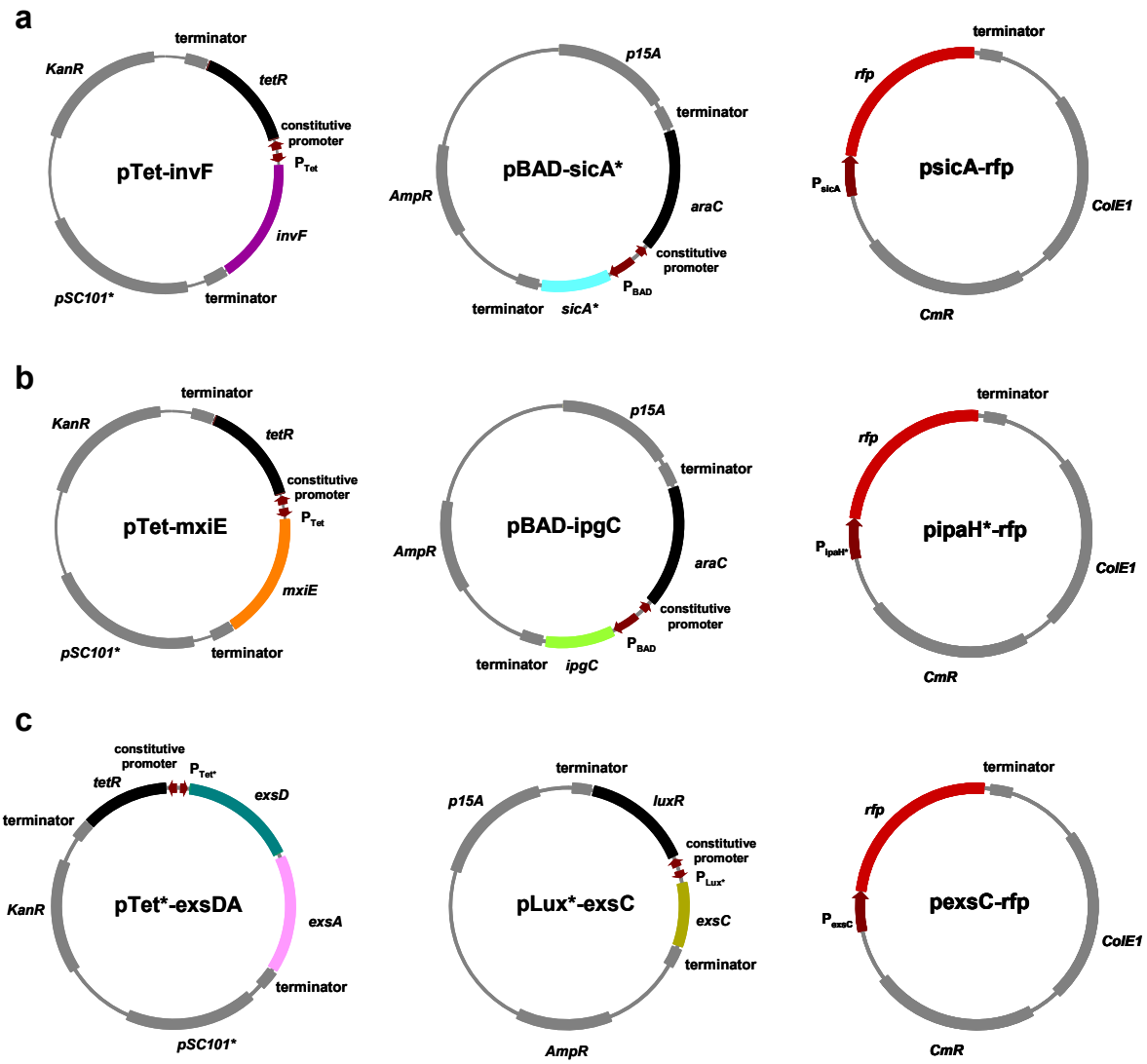

Figure S17: **Plasmids used for 2-D transfer functions and orthogonality test. (a)** Plasmids constructed using *Salmonella* parts. **(b)** Plasmids constructed using *Shigella* parts. **(c)** Plasmids constructed using *Pseudomonas* parts.

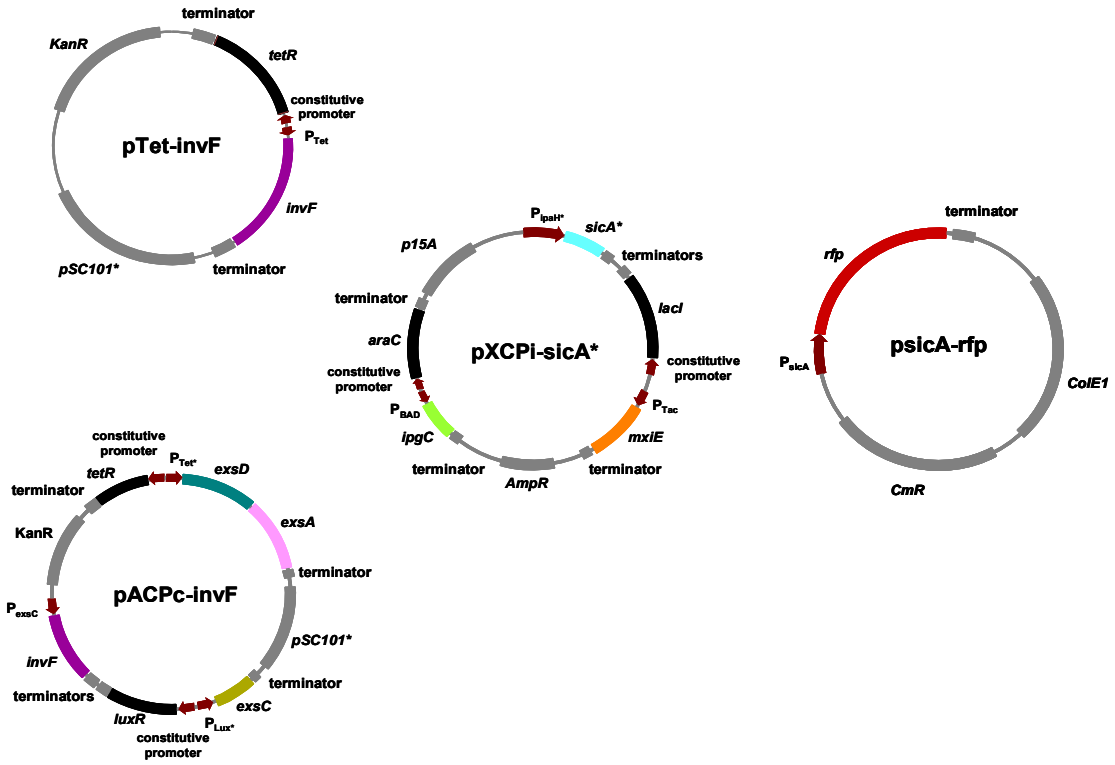

Figure S18: **Plasmids used for the 3- and 4-input AND gates.** The two plasmids pXCPi-sicA* and psicA-rfp are common for both gates, but the 3- and 4-input gate contains pTet-invF and pACPc-invF, respectively.

Table S4. List of genetic parts used in this work.

Part name	Type and source	DNA sequence	Mutations done in this study
sicA	Gene[22]	atggattatcaaaataatgtcagcgaagaacgtgttgcggaaatgatttgggatgccgttagtgaaggcgccacgctaaaagacgttcatgggatccctcaagatatgatggacggtttatatgctcatgcttatgagttttataaccagggacgactggatgaagctgagacgttctttcgtt**t**cttatgcatttatgatttttacaatcccgattacaccatgggactggcggcagtatgccaactgaaaaaacaatttcagaaagcatgtgacctttatgcagtagcgtttacgttacttaaaaatgattatcgccccgttttttttaccgggcagtgtcaattattaatgcgtaaggcagcaaaagccagacagtgttttgaacttgtcaatgaacgtactgaagatgagtctctgcgggcaaaagcgttggtctatctggaggcgctaaaaacggcggagacagagcagcacagtgaacaagaaaaggaataa	
*sicA**	Mutant *sicA*	atggattatcaaaataatgtcagcgaagaacgtgttgcggaaatgatttgggatgccgttagtgaaggcgccacgctaaaagacgttcatgggatccctcaagatatgatggacggtttatatgctcatgcttatgagttttataaccagggacgactggatgaagctgagacgttctttcgtt**a**cttatgcatttatgatttttacaatcccgattacaccatgggactggcggcagtatgccaactgaaaaaacaatttcagaaagcatgtgacctttatgcagtagcgtttacgttacttaaaaatgattatcgccccgttttttttaccgggcagtgtcaattattaatgcgtaaggcagcaaaagccagacagtgttttgaacttgtcaatgaacgtactgaagatgagtctctgcgggcaaaagcgttggtctatctggaggcgctaaaaacggcggagacagagcagcacagtgaacaagaaaaggaataa	The "**t**" of *sicA* (in bold) was mutated to "**a**" by error-prone PCR. This mutation was made to reduce crosstalk between SicA and MxiE.
invF	Gene[28] with new start codon	atgctaaatacgcaggaagtacttaaagaaggagagaagcggaaaatccgcagcccggaagcatggtttatacagacgtgttccgcgcaaaagctgcat**atg**tcattttctgaaagccgacacaatgaaaattgcctgattcaggaaggcgcgctgctttttttgcgagcaggccgttgtcgcaccagtatcaggagacctggtttttcgaccgttaaaaattgaagtactcagcaaattactggcatttatcgatggcgcaggattagtggacacgacatatgctgaatccgataaatgggttttgctgagtcctgagtttcgcgctatttggcaagatcgtaaacgctgcgagtactggtttttgcagcaaattattacgccttctccggccttcaataaggtactggcgctgttacgaaaaagcgagagttactggttggttggctatttactcgctcagtcaaccagcggcaacacgatgagaatgctgggagaagactatggcgtttcttatacccatttttcgtcgtttgtgcagcagagcgttgggcggaaaagcgaagagtgaattacgaaactggcgtatggcgcaatcgctgctgaatagtgtagaa	The annotated start codon (the "**atg**" in bold) was confirmed to be incorrect and a correct upstream start codon was found.

		ggccacgagaacatcacccaattagccgttaatcatggttactcatcgccttcacatttttctagtgagat caaagagctgatcggcgtttcgccgcggaaattatcaaatattattcaattggcagacaaatga	
psicA	Promoter[22]	ccacaagaaacgaggtacggcattgagccgcgtaaggcagtagcgatgtattcattgggcgttttttg aatgttcactaaccaccgtcggggtttaataactgca	
ipgC	Gene[29]	atgtctttaaatatcaccgaaaatgaaagcatctctactgcagtaattgatgcaattaactctggcgctac actgaaagatattaatgcaattcctgatgatatgatggatgacatttattcatatgcttatgacttttacaac aaaggaagaatagaggaagctgaagttttcttcaggtttttatgtatatacgacttttacaatgtagacta cattatgggactcgcagctatttatcagataaaagaacagttccaacaagcagcagacctttatgctgt cgcttttgcattaggaaaaaatgactatacaccagtattccatactggacaatgtcagcttcggttgaaa gccccctaaaagctaaagagtgcttcgaactcgtaattcaacacagcaatgatgaaaaattaaaaata aaagcacaatcatacttggacgcaattcaggatatcaaggagtaa	
mxiE	Gene[1, 29] with codon optimization	**a**tgagtaaatataaaggcctgaacaccagcaacatgttctacatctacagctctggtcatgaaccggt gaacgttgaactggtgaaagataaagaacgtaacatcatcgaactggcaccggcgtggaaagg**ct ttttcttt**gtgcgtaaccagaacatcaaattcagcgataacgttaactaccactaccgcttcaacat caactcttgcgcaaaattcctggcgttttgggattattttagcggcgccctggttgaacattctcacgca gaaaaatgcatccatttctaccacgaaaacgatctgcgtgatagctgtaatacggaatctatgctggat aaactgatgctgcgcttcatttttagtagcgatcagaacgtgtctaatgccctggcaatgatccgtatga ccgaaagttatcatctggttctgtacctgctgcgtacgattgaaaaagaaaaagaagtgcgcatcaaa agcctgaccgaacactatggcgtttctgaagcgtactttcgtagtctgtgtcgcaaagcgctgggtgcc aaagtgaaagaacagctgaacacgtggcgcctggtgaatggcctgctggatgttttcctgcataacca gaccattacgagcgcggccatgaacaatggttatgcgtctaccagtcacttcagcaatgaaattaaaa cgcgtctgggctttagtgcccgcgaactgagcaacatcaccttcctggtgaagaaaattaatgaaaaa atctaa	The wild-type gene has "**tttttttt**" sequence region (in bold). One more "t" was added to make "**ttttttttt**" and then the entire gene was codon optimized (to make **ctttttcttt**) by GenScript (Piscataway, NJ). The additional "**t**" was added to make this ORF in-frame. In addition, the wild-type gene starts with "**g**" and this synthetic gene starts with "**a**" (in bold).
pipaH	Promoter[29]	gcgaaaatgacatcaaaaacgccattaacctgatgttctggggaatataaatgtcaggctagggtcaa aaatcgtggcgttgacaaaatggctgcgttacgtcattgagcatatccaggactggccggcaaaccg ggtacgcgatctgttgccttggaaagttgatctgacctctcagtaaatatcaatacggttctgacgagcc gcttaccgttcaaatatgaagtacgatgtttaactaaccgaaaaacaagaacaatacggtgcaaacag gccattcacggttaactgaaacagtatcgtttttttacagccaattttgtttatccttatta**ta**ataaaaaag tgct	
*pipaH**	Promoter with mutation	gcgaaaatgacatcaaaaacgccattaacctgatgttctggggaatataaatgtcaggctagggtcaa aaatcgtggcgttgacaaaatggctgcgttacgtcattgagcatatccaggactggccggcaaaccg ggtacgcgatctgttgccttggaaagttgatctgacctctcagtaaatatcaatacggttctgacgagcc gcttaccgttcaaatatgaagtacgatgtttaactaaccgaaaaacaagaacaatacggtgcaaacag gccattcacggttaactgaaacagtatcgtttttttacagccaattttgtttatccttatta**ag**ataaaaaa gtgct	The "**ta**" of pipaH (in bold) was mutated to "**ag**" by saturation mutagenesis. This mutation was made to reduce leaky expression of pipaH.
exsC	Gene[30]	atggatttaacgagcaaggtcaaccgactgcttgccgagttcgcaggccgtatcggttttgccttccctg tccctcgacgaggagggcatggcgagcctcctgttcgacgaacaggtgggcgtcaccctgttgctg ctcgccgagcgcgagcgtctgttgctggaggccgatgtggcgggcatcgatgtgctgggcgaggg gatctttcgccagctcgccagcttcaaccgccattggcaccgtttcgatctgcatttcggcttcgacga gctgaccggcaaggtccagttgtatgcgcagattctcgcagcgcaactgaccctcgaatgcttcgag gcgaccttggccaatctgctcgatcacgccgagttctggcagcgcctgctgccgtgcgacagtgatc gcgaggcggtcgctgcggtcggcatgagggtttga	
exsD	Gene[30]	atggagcaggaagacgataagcagtactcccgagaagcggtgttcgctggcaggcgggtatccgt ggtgggctcggacgcccgctcgcggggtcgggtgccgggttacgcatcgagcagtttgtatcgtga gtccggaatcatcagtgcgcggcaactggcgttgctgcagcggatgctgccgcgcctgcggctgga gcaactgttccgctgcgagtggttgcagcagcgcctggcgcgcggcctggcgctggggcgcgaag aggtgcggcagattctcctctgcgcggcgcaggacgacgacggctggtgctccgaactgggcgac cgggtcaacctcgccgtgccgcagtcgatgatcgactgggtcctgctgccggtctatggctggtggg aaagcctgctcgaccaggcgatccccggctggcgcctgtcgctggtggagctggagacccagtcc cggcaactgcgagtcaagtccgaattctggtcccgcgtggccgagctggagccggagcaggcccg cgaggaactggccagggtcgccaagtgccaggcgcgcacccaggaacaggtggccgaactggc cggcaagctggagacggcttcggcactggcgaagagcgcctggccgaactggcagcggggcatg gcgacgctgctcgccagcggcgggctggccggcttcgagccgatccccgaggtcctcgaatgcct ctggcaacctctctgccggctggacgacgacgtcggcgcggcggacgccgtccaggcctggctgc acgaacgcaacctgtgccaggcacaggatcacttctactggcagagctga	
exsA	Gene[30]	atgcaaggagccaaatctcttggccgaaagcagataacgtcttgtcattggaacattccaactttcgaa tacagggtaaacaaggaagagggcgtatatgttctgctcgagggcgaactgaccgtccaggacatc gattccacttttgcctggcgcctggcgagttgcttttcgtccgccgcggaagctatgtcgtaagtacca agggaaaggacagccgaatactctggattccattatctgcccagtttctacaaggcttcgtccagcgct tcggcgcgctgttgagtgaagtcgagcgttgcgacgagcccgtgccgggcatcatcgcgttcgctg ccacgcctctgctggccggttgcgtcaaggggttgaaggaattgcttgtgcatgagcatccgccgat gctcgcctgcctgaagatcgaggagttgctgatgctcttcgcgttcagtccgcaggggccgctgctg atgtcggtcctgcggcaactgagcaaccggcatgtcgagcgtctgcagctattcatggagaagcact acctcaacgagtggaagctgtccgacttctcccgcgagttcggcatggggctgaccaccttcaagga	

		gctgttcggcagtgtctatggggtttcgccgcgcgcctggatcagcgagcggagaatcctctatgcc catcagttgctgctcaacagcgacatgagcatcgtcgacatcgccatggaggcgggcttttccagtca gtcctatttcacccagagctatcgccgccgtttcggctgcacgccgagccgctcgcggcaggggaa ggacgaatgccgggctaaaaataactga
pexsD	Promoter[30]	gaaggacgaatgccgggctaaaaataactgacgtttttgaaagcccggtagcggctgcatgagtag aatcggcccaaat
pexsC	Promoter[30]	gatgtggctttttttcttaaaagaaaagtctctcagtgacaaaagcgatgcatagcccggtgctagcatg cgctgagcttt
phlF	Gene[4] with codon optimization	atggcacgtaccccgagccgtagcagcattggtagcctgcgtagtccgcatacccataaagcaattct gaccagcaccattgaaatcctgaaagaatgtggttatagcggtctgagcattgaaagcgttgcacgtc gtgccggtgcaagcaaaccgaccatttatcgttggtggaccaataaagcagcactgattgccgaagt gtatgaaaatgaaagcgaacaggtgcgtaaatttccggatctgggtagctttaaagccgatctggattt tctgctgcgtaatctgtggaaagtttggcgtgaaaccatttgtggtgaagcatttcgttgtgttattgcag aagcacagctggaccctgcaaccctgacccagctgaaagatcagtttatggaacgtcgtcgtgagat gccgaaaaaactggttgaaaatgccattagcaatggtgaactgccgaaagataccaatcgtgaactg ctgctggatatgatttttggttttgttggtatcgcctgctgaccgaacagctgaccgttgaacaggatatt gaagaatttaccttcctgctgattaatggtgtttgtccgggtacacagcgttaa
pphlF	Synthetic Promoter[5]	tctgattcgttaccaattgacatgatacgaaacgtaccgtatcgttaaggt
rfp	Gene[31]	atggcttcctccgaagacgttatcaaagagttcatgcgtttcaaagttcgtatggaaggttccgttaacg gtcacgagttcgaaatcgaaggtgaaggtgaaggtcgtccgtacgaaggtacgcagaccgctaaac tgaaagttaccaaaggtggtccgctgccgttcgcttgggacatcctgtccccgcagttccagtacggtt ccaaagcttacgttaaacacccggctgacatcccggactacctgaaactgtccttcccggaaggtttc aaatgggaacgtgttatgaacttcgaagacggtggtgttgttaccgttacccaggactcctccctgcaa gacggtgagttcatctacaaagttaaactgcgtggtactaacttcccgtccgacggtccggttatgcag aaaaaaaccatgggttgggaagcttccaccgaacgtatgtacccggaagacggtgctctgaaaggt gaaatcaaaatgcgtctgaaactgaaagacggtggtcactacgacgctgaagttaaaaccacctaca tggctaaaaaaccggttcagctgccgggtgcttacaaaaccgacatcaaactggacatcacctccca caacgaagactacaccatcgttgaacagtacgaacgtgctgaaggtcgtcactccaccggtgctgca gcaaacgacgaaaactacgcttaa
gfp	Gene[22]	atgagtaaaggagaagaacttttcactggagttgtcccaattcttgttgaattagatggtgatgttaatgg gcacaaatttttctgtcagtggagagggtgaaggtgatgcaacatacggaaaacttaccctaaatttatt tgcactactggaaaactacctgttccatggccaacacttgtcactactttgacttatggtgttcaatgctttt caagatacccagatcatatgaaacggcatgactttttcaagagtgccatgcccgaaggttatgtacag gaaagaactatatttttcaaagatgacgggaactataagacacgtgctgaagtcaagtttgaaggtgat acacttgttaatagaatcgagttaaaaggtattgattttaaagaagatggaaacattcttggacacaagtt ggaatacaactataactcacacaatgtatacatcatggcagacaaacaaaagaatggaatcaaagtta acttcaaaattagacacaacattgaagatggaagcgttcaactagcagaccattatcaacaaaatactc caattggcgatggccctgtccttttaccagacaaccattacctgtccacacaatctgccctttcgaaaga tcccaacgaaaagagagaccacatggtccttcttgagtttgtaacagctgctgggattacacatggcat ggatgaactatacaaaaggcctgcagcaaacgacgaaaactacgcttaa
araC	Gene[22]	atggctgaagcgcaaaatgatcccctgctgccgggatactcgtttaatgcccatctggtggcgggttta acgccgattgaggccaacggttatctcgatttttttatcgaccgaccgctgggaatgaaaggttatattc tcaatctcaccattcgcggtcaggggtggtgaaaaatcagggacgagaatttgtttgccgaccgggt gatattttgctgttcccgccaggagagattcatcactacggtcgtcatccggaggctcgcgaatggtat caccagtgggtttactttcgtccgcgcgcctactggcatgaatggcttaactggccgtcaatatttgcca atacggggttctttcgcccggatgaagcgcaccagccgcatttcagcgacctgtttgggcaaatcatt aacgccgggcaagggggaagggcgctattcggagctgctggcgataaatctgcttgagcaattgttac tgcggcgcatggaagcgattaacgagtcgctccatccaccgatggataatcgggtacgcgaggctt gtcagtacatcagcgatcacctggcagacagcaattttgatatcgccagcgtcgcacagcatgtttgct tgtcgccgtcgcgtctgtcacatcttttccgccagcagttagggattagcgtcttaagctggcgcgagg accaacgtatcagccaggcgaagctgcttttgagcaccacccggatgcctatcgccaccgtcggtcg caatgttggttttgacgatcaactctatttctcgcgggtatttaaaaaatgcaccggggccagcccgag cgagttccgtgccggttgtgaagaaaaagtgaatgatgtagccgtcaagttgtcataa
lacI	Gene[32]	gtgaaaccagtaacgttatacgatgtcgcagagtatgccggtgtctcttatcagaccgtttcccgcgtg gtgaaccaggccagccacgtttctgcgaaaacgcgggaaaaagtggaagcggcgatggcggagc tgaattacattcccaaccgcgtggcacaacaactggcgggcaaacagtcgttgctgattggcgttgcc acctccagtctggccctgcacgcgccgtcgcaaattgtcgcggcgattaaatctcgcgccgatcaact gggtgccagcgtggtggtgtcgatggtagaacgaagcggcgtcgaagcctgtaaagcggcggtgc acaatcttctcgcgcaacgcgtcagtgggctgatcattaactatccgctggatgaccaggatgccattg ctgtggaagctgcctgcactaatgttccggcgttatttcttgatgtctctgaccagacacccatcaacag tattattttctcccatgaagacggtacgcgactgggcgtggagcatctggtcgcattgggtcaccagca aatcgcgctgttagcgggcccattaagttctgtctcggcgcgtctgcgtctggctggctggcataaata tctcactcgcaatcaaattcagccgatagcggaacgggaaggcgactggagtgccatgtccggttttc aacaaaccatgcaaatgctgaatgagggcatcgttcccactgcgatgctggttgccaacgatcagat ggcgctgggcgcaatgcgcgccattaccgagtccgggctgcgcgttggtgcggatatctcggtagt gggatacgacgataccgaagacagctcatgttatatcccgccgttaaccaccatcaaacaggattttc gcctgctggggcaaaccagcgtggaccgcttgctgcaactctctcagggccaggcggtgaagggc aatcagctgttgcccgtctcactggtgaaaagaaaaaccaccctggcgcccaatacgcaaaccgcct

		ctccccgcgcgttggccgattcattaatgcagctggcacgacaggtttcccgactggaaagcgggca gtga	
luxR	Gene[33]	atgaaaaacataaatgccgacgacacatacagaataattaataaaattaaagcttgtagaagcaataat gatattaatcaatgcttatctgatatgactaaaatggtacattgtgaatattatttactcgcgatcatttatcc tcattctatggttaaatctgatatttcaatcctagataattaccctaaaaaatggaggcaatattatgatga cgctaatttaataaaatatgatcctatagtagattattctaactccaatcattcaccaattaattggaatatat ttgaaaacaatgctgtaaataaaaaatctccaaatgtaattaaagaagcgaaaacatcaggtcttatcac tgggtttagtttccctattcatacggctaacaatggcttcggaatgcttagttttgcacattcagaaaaag acaactatatagatagtttatttttacatgcgtgtatgaacataccattaattgttccttctctagttgataatt atcgaaaaataaatatagcaaataataaatcaaacaacgatttaaccaaaagagaaaaagaatgtttag cgtgggcatgcgaaggaaaaagctcttgggatatttcaaaaatattaggttgcagtgagcgtactgtca ctttccatttaaccaatgcgcaaatgaaactcaatacaacaaaccgctgccaaagtatttctaaagcaat tttaacaggagcaattgattgcccatactttaaaaattaa	
tetR	Gene[34]	atgtccagattagataaaagtaaagtgattaacagcgcattagagctgcttaatgaggtcggaatcgaa ggtttaacaacccgtaaactcgcccagaagctaggtgtagagcagcctacattgtattggcatgtaaa aaataagcgggctttgctcgacgccttagccattgagatgttagataggcaccatactcacttttgccct ttagaaggggaaagctggcaagatttttacgtaataacgctaaaagttttagatgtgctttactaagtca tcgcgatggagcaaaagtacatttaggtacacggcctacagaaaaacagtatgaaactctcgaaaat caattagccttttatgccaacaaggtttttcactagagaatgcattatatgcactcagcgctgtggggca ttttacttaggttgcgtattggaagatcaagagcatcaagtcgctaaagaagaaagggaaacacctac tactgatagtatgccgccattattacgacaagctatcgaattatttgatcaccaaggtgcagagccagc cttcttattcggccttgaattgatcatatgcggattagaaaaacaacttaaatgtgaaagtgggtcctaa	
pBAD	Promoter[22]	agaaaccaattgtccatattgcatcagacattgccgtcactgcgtcttttactggctcttctcgctaacca aaccggtaaccccgcttattaaaagcattctgtaacaaagcgggaccaaagccatgacaaaaacgc gtaacaaaagtgtctataatcacggcagaaaagtccacattgattatttgcacggcgtcacactttgcta tgccatagcatttttatccataagattagcggatcctacctg	
pTac	Promoter[32]	caatgcttctggcgtcaggcagccatcggaagctgtggtatggctgtgcaggtcgtaaatcactgcat aattcgtgtcgctcaaggcgcactcccgttctggataatgtttttgcgccgacatcataacggttctgg caaatattctgaaatgagctgttgacaattaatcatcggctcgtataatgtgtggaattgtgagcgctcac aatttcacacaggaaaca	
pLux	Promoter[33]	acctgtaggatcgtacaggtttacgcaagaaaatggtttgtta**tag**tcgaataaa	
*pLux**	Promoter with mutation	acctgtaggatcgtacaggtttacgcaagaaaatggtttgtta**ctt**tcgaataaa	The "**tag**" of *pLux* (in bold) was mutated to "**ctt**" by saturation mutagenesis. This mutation was made to reduce leaky expression of *pLux*.
pTet	Promoter[34]	tttttccctatcagtgatagagattgacatccctatcagtgatagagatactgagcac**ctcg**	
*pTet**	Promoter with mutation	tttt**cagcaggacgcactgacc**tccctatcagtgatagagattgacatccctatcagtg atagagatactgagcac**atat**	To reduce leaky expression of *pTet*, the "**ctcg**" of *pTet* (in bold) was mutated to "**atat**" and the "**cagcaggacgcactgacc**" was inserted.

Table S5. List of strains used in this work[a].

Name	Input promoters	Output promoter	Plasmids
AND2	P_{Tet}, P_{BAD}	P_{sicA}	pTet-invFORF1, pBAD-sicA, psicA-rfp
AND5	P_{Tet}, P_{BAD}	P_{sicA}	pTet-invFORF2, pBAD-sicA, psicA-rfp
AND6	P_{Tet}, P_{BAD}	P_{sicA}	pTet-invFORF3, pBAD-sicA, psicA-rfp
AND7	P_{Tet}, P_{BAD}	P_{sicA}	pTet-invFORF4, pBAD-sicA, psicA-rfp
AND8	P_{Tet}, P_{BAD}	P_{sicA}	pTet-invFORF5, pBAD-sicA, psicA-rfp
AND9	P_{Tet}, P_{BAD}	P_{sicA}	pTet-invFORF6, pBAD-sicA, psicA-rfp
AND11	P_{Tet}, P_{BAD}	P_{sicA}	pTet-invFORF6*, pBAD-sicA, psicA-rfp
AND12	P_{Tet}, P_{BAD}	P_{sicA}	pTet-invFORF1*, pBAD-sicA, psicA-rfp
AND18	P_{Tet}, P_{BAD}	P_{sicA}	pTet-invF, pBAD-sicA, psicA-rfp

AND19	P_{Tet}, P_{BAD}	P_{sycB}	pTet-ysaE, pBAD-sycB, psycB-rfp
AND20	P_{Tet}, P_{BAD}	P_{ipaH}	pTet-mxiERBS, pBAD-ipgCRBS, pipaH-rfp
AND21	P_{Tet}	P_{sycB}	pTet-ysaE, psycB-rfp
AND22	P_{BAD}	P_{sycB}	pBAD-sycB, psycB-rfp
AND24	P_{Tet}, P_{BAD}	P_{ipaH*}	pTet-mxiE, pBAD-ipgC, pipaH*-rfp
AND32	P_{Tet}, P_{BAD}	P_{sicA}	pTet-invF, pBAD-ipgC, psicA-rfp
AND33	P_{Tet}, P_{BAD}	P_{ipaH*}	pTet-invF, pBAD-ipgC, pipaH*-rfp
AND36	P_{Tet}, P_{BAD}	P_{sicA}	pTet-mxiE, pBAD-ipgC, psicA-rfp
AND37	P_{Tet}, P_{BAD}	P_{sicA}	pTet-invF, pBAD-sicA*, psicA-rfp
AND38	P_{Tet}, P_{BAD}	P_{ipaH*}	pTet-invF, pBAD-sicA*, pipaH*-rfp
AND39	P_{Tet}, P_{BAD}	P_{sicA}	pTet-mxiE, pBAD-sicA*, psicA-rfp
AND40	P_{Tet}, P_{BAD}	P_{ipaH*}	pTet-mxiE, pBAD-sicA*, pipaH*-rfp
AND42[b]	P_{Tet}, P_{BAD}, P_{Tac}	P_{sicA}	pTet-invF, pXCPi-sicA*, psicA-rfp
AND47	P_{Tet}, P_{Lux}	P_{exsD}	pTet-exsDA, pLux-exsC, pexsD-rfp
AND50	P_{Tet*}, P_{Lux*}	P_{exsD}	pTet*-exsDA, pLux*-exsC, pexsD-rfp
AND53	P_{Tet}, P_{Lux*}	P_{sicA}	pTet-invF, pLux*-exsC, psicA-rfp
AND54	P_{Tet}, P_{Lux*}	P_{ipaH*}	pTet-invF, pLux*-exsC, pipaH*-rfp
AND58	P_{Tet}, P_{Lux*}	P_{sicA}	pTet-mxiE, pLux*-exsC, psicA-rfp
AND59	P_{Tet}, P_{Lux*}	P_{ipaH*}	pTet-mxiE, pLux*-exsC, pipaH*-rfp
AND61	P_{Tet*}, P_{BAD}	P_{sicA}	pTet*-exsDA, pBAD-sicA*, psicA-rfp
AND62	P_{Tet*}, P_{BAD}	P_{ipaH*}	pTet*-exsDA, pBAD-sicA*, pipaH*-rfp
AND64	P_{Tet*}, P_{BAD}	P_{sicA}	pTet*-exsDA, pBAD-ipgC, psicA-rfp
AND65	P_{Tet*}, P_{BAD}	P_{ipaH*}	pTet*-exsDA, pBAD-ipgC, pipaH*-rfp
AND67	P_{Tet*}, P_{Lux*}	P_{sicA}	pTet*-exsDA, pLux*-exsC, psicA-rfp
AND68	P_{Tet*}, P_{Lux*}	P_{ipaH*}	pTet*-exsDA, pLux*-exsC, pipaH*-rfp
AND72	P_{Tet}, P_{BAD}	P_{exsC}	pTet-invF, pBAD-ipgC, pexsC-rfp
AND73	P_{Tet}, P_{Lux*}	P_{exsC}	pTet-invF, pLux*-exsC, pexsC-rfp
AND74	P_{Tet}, P_{BAD}	P_{exsC}	pTet-mxiE, pBAD-sicA*, pexsC-rfp
AND75	P_{Tet}, P_{Lux*}	P_{exsC}	pTet-mxiE, pLux*-exsC, pexsC-rfp
AND76	P_{Tet*}, P_{BAD}	P_{exsC}	pTet*-exsDA, pBAD-sicA*, pexsC-rfp
AND77	P_{Tet*}, P_{BAD}	P_{exsC}	pTet*-exsDA, pBAD-ipgC, pexsC-rfp
AND78	P_{Tet}, P_{BAD}	P_{exsC}	pTet-invF, pBAD-sicA*, pexsC-rfp
AND79	P_{Tet}, P_{BAD}	P_{exsC}	pTet-mxiE, pBAD-ipgC, pexsC-rfp
AND80	P_{Tet*}, P_{Lux*}	P_{exsC}	pTet*-exsDA, pLux*-exsC, pexsC-rfp
AND81[c]	P_{Tet*}, P_{BAD}, P_{Tac}, P_{Lux*}	P_{sicA}	pACPc-invF, pXCPi-sicA*, psicA-rfp
NAND1[d]	P_{Tet}, P_{BAD}	P_{phlF}	pTet-invF, pBAD-sicA*, pNotP-rfp

a. The host strain is *E. coli* DH10B.
b. The strain has additional output promoter (P_{ipaH*}) acting as input promoter as well.
c. The strain has additional output promoters ($P_{ipaH*}$and P_{exsC}) acting as input promoters as well.
d. The strain has additional output promoter (P_{sicA}) acting as input promoter as well.

IX. References

1. Penno, C., Sansonetti, P. & Parsot, C. Frameshifting by transcriptional slippage is involved in production of MxiE, the transcription activator regulated by the activity of the type III secretion apparatus in Shigella flexneri. *Mol Microbiol* **56**, 204-214 (2005).

2. Brutinel, E.D., Vakulskas, C.A., Brady, K.M. & Yahr, T.L. Characterization of ExsA and of ExsA-dependent promoters required for expression of the Pseudomonas aeruginosa type III secretion system. *Mol Microbiol* **68**, 657-671 (2008).
3. Davis, J.H., Rubin, A.J. & Sauer, R.T. Design, construction and characterization of a set of insulated bacterial promoters. *Nucleic acids research* **39**, 1131-1141 (2011).
4. Bangera, M.G. & Thomashow, L.S. Identification and characterization of a gene cluster for synthesis of the polyketide antibiotic 2,4-diacetylphloroglucinol from Pseudomonas fluorescens Q2-87. *Journal of bacteriology* **181**, 3155-3163 (1999).
5. Abbas, A. et al. Characterization of interactions between the transcriptional repressor PhlF and its binding site at the phlA promoter in Pseudomonas fluorescens F113. *Journal of bacteriology* **184**, 3008-3016 (2002).
6. Ackers, G.K., Johnson, A.D. & Shea, M.A. Quantitative model for gene regulation by lambda phage repressor. *Proceedings of the National Academy of Sciences of the United States of America* **79**, 1129-1133 (1982).
7. Bintu, L. et al. Transcriptional regulation by the numbers: applications. *Curr Opin Genet Dev* **15**, 125-135 (2005).
8. Bintu, L. et al. Transcriptional regulation by the numbers: models. *Curr Opin Genet Dev* **15**, 116-124 (2005).
9. Collins, C.H., Arnold, F.H. & Leadbetter, J.R. Directed evolution of Vibrio fischeri LuxR for increased sensitivity to a broad spectrum of acyl-homoserine lactones. *Mol Microbiol* **55**, 712-723 (2005).
10. Grigorova, I.L., Phleger, N.J., Mutalik, V.K. & Gross, C.A. Insights into transcriptional regulation and sigma competition from an equilibrium model of RNA polymerase binding to DNA. *Proceedings of the National Academy of Sciences of the United States of America* **103**, 5332-5337 (2006).
11. Passador, L. et al. Functional analysis of the Pseudomonas aeruginosa autoinducer PAI. *Journal of bacteriology* **178**, 5995-6000 (1996).
12. Buttner, C.R., Sorg, I., Cornelis, G.R., Heinz, D.W. & Niemann, H.H. Structure of the Yersinia enterocolitica type III secretion translocator chaperone SycD. *J Mol Biol* **375**, 997-1012 (2008).
13. Job, V., Mattei, P.J., Lemaire, D., Attree, I. & Dessen, A. Structural basis of chaperone recognition of type III secretion system minor translocator proteins. *J Biol Chem* **285**, 23224-23232 (2010).
14. Lunelli, M., Lokareddy, R.K., Zychlinsky, A. & Kolbe, M. IpaB-IpgC interaction defines binding motif for type III secretion translocator. *Proceedings of the National Academy of Sciences of the United States of America* **106**, 9661-9666 (2009).
15. Darwin, K.H. & Miller, V.L. Type III secretion chaperone-dependent regulation: activation of virulence genes by SicA and InvF in Salmonella typhimurium. *The EMBO journal* **20**, 1850-1862 (2001).
16. Thibault, J., Faudry, E., Ebel, C., Attree, I. & Elsen, S. Anti-activator ExsD forms a 1:1 complex with ExsA to inhibit transcription of type III secretion operons. *The Journal of biological chemistry* **284**, 15762-15770 (2009).
17. Lykken, G.L., Chen, G., Brutinel, E.D., Chen, L. & Yahr, T.L. Characterization of ExsC and ExsD self-association and heterocomplex formation. *Journal of bacteriology* **188**, 6832-6840 (2006).

18. Vogelaar, N.J., Jing, X., Robinson, H.H. & Schubot, F.D. Analysis of the crystal structure of the ExsC.ExsE complex reveals distinctive binding interactions of the Pseudomonas aeruginosa type III secretion chaperone ExsC with ExsE and ExsD. *Biochemistry* **49**, 5870-5879 (2010).
19. Brutinel, E.D., Vakulskas, C.A. & Yahr, T.L. Functional domains of ExsA, the transcriptional activator of the Pseudomonas aeruginosa type III secretion system. *Journal of bacteriology* **191**, 3811-3821 (2009).
20. Vakulskas, C.A., Brutinel, E.D. & Yahr, T.L. ExsA recruits RNA polymerase to an extended -10 promoter by contacting region 4.2 of sigma-70. *Journal of bacteriology* **192**, 3597-3607 (2010).
21. Hooshangi, S., Thiberge, S. & Weiss, R. Ultrasensitivity and noise propagation in a synthetic transcriptional cascade. *Proc. Natl. Acad. Sci. USA* **102**, 3581-3586 (2005).
22. Temme, K. et al. Induction and relaxation dynamics of the regulatory network controlling the type III secretion system encoded within Salmonella pathogenicity island 1. *Journal of molecular biology* **377**, 47-61 (2008).
23. Gibson, D.G. et al. Enzymatic assembly of DNA molecules up to several hundred kilobases. *Nat Methods* **6**, 343-345 (2009).
24. Siegele, D.A. & Hu, J.C. Gene expression from plasmids containing the araBAD promoter at subsaturating inducer concentrations represents mixed populations. *Proceedings of the National Academy of Sciences of the United States of America* **94**, 8168-8172 (1997).
25. Anderson, J.C., Voigt, C.A. & Arkin, A.P. Environmental signal integration by a modular AND gate. *Mol. Syst. Biol.* **3**, 133 (2007).
26. Temme, K., Zhao, D. & Voigt, C.A. Refactoring the nitrogen fixation gene cluster from Klebsiella oxytoca. *Proceedings of the National Academy of Sciences of the United States of America* **109**, 7085-7090 (2012).
27. Kelly, J.R. et al. Measuring the activity of BioBrick promoters using an in vivo reference standard. *Journal of biological engineering* **3**, 4 (2009).
28. McClelland, M. et al. Complete genome sequence of Salmonella enterica serovar Typhimurium LT2. *Nature* **413**, 852-856 (2001).
29. Buchrieser, C. et al. The virulence plasmid pWR100 and the repertoire of proteins secreted by the type III secretion apparatus of Shigella flexneri. *Mol Microbiol* **38**, 760-771 (2000).
30. Stover, C.K. et al. Complete genome sequence of Pseudomonas aeruginosa PAO1, an opportunistic pathogen. *Nature* **406**, 959-964 (2000).
31. Moon, T.S. et al. Construction of a genetic multiplexer to toggle between chemosensory pathways in Escherichia coli. *Journal of molecular biology* **406**, 215-227 (2011).
32. Dykxhoorn, D.M., St Pierre, R. & Linn, T. A set of compatible tac promoter expression vectors. *Gene* **177**, 133-136 (1996).
33. Canton, B., Labno, A. & Endy, D. Refinement and standardization of synthetic biological parts and devices. *Nat. Biotechnol.* **26**, 787-793 (2008).
34. Lutz, R. & Bujard, H. Independent and tight regulation of transcriptional units in Escherichia coli via the LacR/O, the TetR/O and AraC/I1-I2 regulatory elements. *Nucleic acids research* **25**, 1203-1210 (1997).